(2)

A STUDY OF HELIUM : ARGON : ETHANE GAS MIXTURES USED IN DRIFT CHAMBERS FOR LARGE ACCEPTANCE SPECTROMETERS IN HIGH MAGNETIC FIELDS

BY

JYUJI D. HEWITT

Master of Science in Systems Management, Florida Institute of Technology, 1988

Bachelor of Science, University of Maine - Orono, 1978

THESIS

Submitted to the University of New Hampshire
in Partial Fulfillment of
the Requirements for the Degree of

Master of Science

in

Physics

December, 1990

REPORT DOCUMENTATION PAGE

Form Approved
OMB No. 0704-0188

1. AGENCY USE ONLY *(Leave Blank)*	2. REPORT DATE	3. REPORT TYPE AND DATES COVERED
	7/12/90	Final

4. TITLE AND SUBTITLE

A STUDY OF HELIUM:ARGON:ETHANE GAS MIXTURES USED IN DRIFT CHAMBERS FOR LARGE ACCEPTANCE SPECTROMETERS IN HIGH MAGNETIC FIELDS

5. FUNDING NUMBERS

6. AUTHOR(S)

MAJOR Jyuji D. Hewitt

7. PERFORMING ORGANIZATION NAME(S) AND ADDRESS(ES)

University of New Hampshire
Department of Physics
Demeritt Hall
Durham, New Hampshire 03824

8. PERFORMING ORGANIZATION REPORT NUMBER

9. SPONSORING/MONITORING AGENCY NAME(S) AND ADDRESS(ES)

Department of the Army
HQDA, TAPA
200 Stoval Street
Alexandria, Va

10. SPONSORING/MONITORING AGENCY REPORT NUMBER

11. SUPPLEMENTARY NOTES

12a. DISTRIBUTION/AVAILABILITY STATEMENT

12b. DISTRIBUTION CODE

13. ABSTRACT *(Maximum 200 words)*

For today's large acceptance spectrometers, precise knowledge of electrons in gases and magnetic fields is required for particle track reconstruction. Measurements under a variety of conditions must be performed in order to accurately model these processes with software simulations such as GARFIELD. At Brookhaven National Laboratory, a prototype drift chamber, constructed at the Continuous Electron Beam Accelerator Facility (CEBAF), incorporating a hex-cell wire pattern, was filled with helium:argon:ethane and tested in a high magnetic field. Additionally, this without the magnetic field. The results of these tests are compared and indicate little change in the drift velocity of this gas mixture in and out of a high magnetic field.

14. SUBJECT TERMS	15. NUMBER OF PAGES
Drift Chambers, drift velocity and diffusion of gases,	82
	16. PRICE CODE

17. SECURITY CLASSIFICATION OF REPORT	18. SECURITY CLASSIFICATION OF THIS PAGE	19. SECURITY CLASSIFICATION OF ABSTRACT	20. LIMITATION OF ABSTRACT
UNCLAS	UNCLAS	UNCLAS	

This thesis has been examined and approved.

Thesis director, F. William Hersman,
Associate Professor of Physics

John F. Dawson, Professor of Physics

Dawn C. Meredith, Assistant Professor of Physics

7 Dec 1990
Date

To my wife Susan, and my sons Matthew and Andrew

ACKNOWLEDGEMENTS

This thesis culminates for me nearly three years of some of the most difficult work I have ever done. Not only has the experience been extremely satisfying, but I have learned much in our world of physics. Through these years, a number of people have assisted me, encouraged me, and supported me.

First of all, I am grateful to Major (P) Thomas Bortner, my Ordnance branch career development officer. Through his suggestion, I applied for the Army's Advanced Civil Schooling Program and was accepted.

I entered the University of New Hampshire after being out of school over ten years as a former chemistry major. Nonetheless, I faced great challenges as I returned to academia. The faculty here was truly understanding and supportive of my unique background. I especially want to thank Professor John Mulhern for his kind words and open door for the many physics questions I posed.

To complete the work on this thesis, I needed the helping hands of many truly outstanding people. The experiment could not be run without the help of several talented scientists and friends at the Continuous Electron Beam Accelerator Facility. I specifically want to acknowledge the practical assistance and advice of Steve Christo (Dr. Detector), his office partner Chris Cuevas, Doug Tilles, and Shouben Zhou. Their support was immeasurable. I also want to thank Doctors Mac Mestayer and Stan Majewski for their advice and instruction on drift chambers and gases used in them.

A special thank-you is in order for Professor Rory Miskimen of the University of Massachusetts. Dr. Miskimen's originally proposed experiment provided the opportunity for me to do my tests.

Here at the University of New Hampshire, our own Nuclear Physics Group assisted in many ways. Dr. Wooyoung Kim, Norman Fontaine, Vance Pomeroy and

Lynette Gelinas helped me purchase, build, and test the drift chamber here. Mike Herrick, the department's machinist, often bent over backwards to assist my cause.

Of course my thesis committee was always available to provide me direction, advice, and encouragement. Professor John Dawson helped to open my eyes in problem solving. Professor Dawn Meredith helped to make the both the computer and the computer programs less intimidating and more useful to me and more importantly, provided a soft touch to the sometimes harsh world of physics. Of course, my thesis director, Professor Bill Hersman understood how to maximize my short time here and make it the most meaningful and educational. I found his experience with experimental nuclear physics most beneficial.

Finally, I must thank my support group. My parents instilled in me the values of hard work and persistence. My in-laws helped keep my household in order when time and studies spread me a little thin. Most of all, I thank my wife Susan for always doing the little extras, like giving a little more love when I needed it and more profoundly, when I thought I didn't need it.

TABLE OF CONTENTS

LIST OF TABLES

LIST OF FIGURES

ABSTRACT

A STUDY OF HELIUM : ARGON : ETHANE GAS MIXTURES USED IN DRIFT CHAMBERS FOR LARGE ACCEPTANCE SPECTROMETERS IN HIGH MAGNETIC FIELDS

by

Jyuji D. Hewitt
University of New Hampshire, December, 1990

For today's proposed large acceptance spectrometers, precise knowledge of electrons in gases and magnetic fields is required for particle track reconstruction. Measurements under a variety of conditions must be performed in order to accurately model these processes with software simulations such as GARFIELD. At Brookhaven National Laboratory, a prototype drift chamber, constructed at the Continuous Electron Beam Accelerator Facility (CEBAF), incorporating a hex-cell wire pattern, was filled with helium:argon:ethane and tested in a high magnetic field. Additionally, this drift chamber was tested without the magnetic field. The results of these tests are compared and indicate little change in the drift velocity of this gas mixture in and out of a high magnetic field.

CHAPTER I

INTRODUCTION

In the current designs of the Large Acceptance Spectrometers, the drift chamber is a significant component. Specifically designed to accurately measure the trajectories of particles, the drift chamber is considered to be a fundamental tracking device in nuclear physics. In principle, it uses the drift time of electrons resulting from an ionizing event in a specifically chosen chamber gas to measure the spatial position of an ionizing particle.

A typical drift chamber set-up, shown in figure 1, consists of a uniform field established between cathode and anode (field and sense) wires.

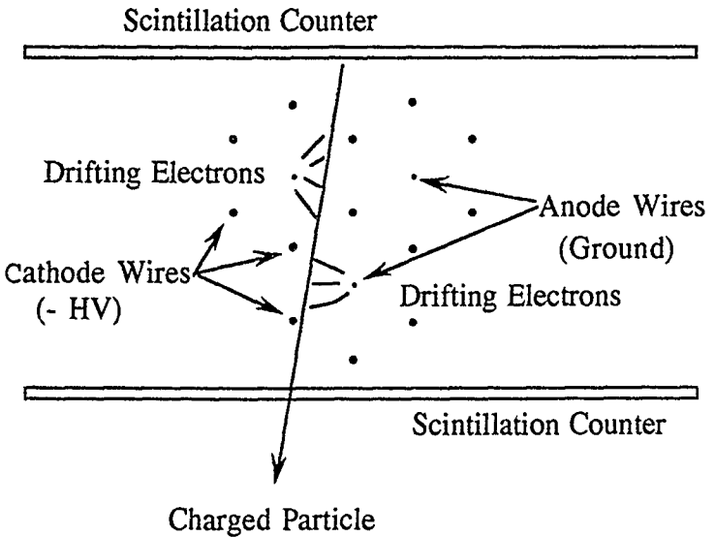

Fig. 1. Basic Operation of the Drift Chamber [Ref. 1].

A charged particle passing through the drift chamber frees electrons from the gas molecules and atoms within the chamber. The scintillation counters, here in a double coincidence set-up, provide the reference time t_0, the arrival of the particle, and t_1, the

arrival of the pulse at the sense wire thus giving the total time of flight for the charged particle. With a trigger of the scintillation counter signalling the arrival of a particle and a known drift velocity, the position of the electron to the sense wire is found by

$$X = \int_{t_0}^{t_1} w(t)\, dt \tag{1.1}$$

where $w(t)$ is the drift velocity [Ref. 2 ,3]. To use this equation, it is most convenient to have a constant drift velocity and a constant electric field. In doing so, a linear relationship is obtained between time and distance $X = w(t_1 - t_0)$.

To establish a constant electric field, the field and sense wires must be arranged so that each sense wire "sees" a uniform field. Hence, each sense wire is surrounded by six field wires in a hexagonal cage. Computer simulations using GARFIELD [Ref. 4] suggest that the field surrounding each sense wire is nearly uniform.

Establishing a gas mixture for a constant drift velocity requires special attention to the drift properties of gases as well as the requirements of the drift chamber. For slower count rates and high spatial resolution, a slow gas is required to minimize timing errors. Helium dominated gases fulfill this requirement and hence it is the objective of this thesis-- to research the effectiveness of helium mixture as a drift chamber gas.

The results of an experiment at Brookhaven National Laboratory studying an argon:ethane:helium mixture as a drift chamber gas are the core of this thesis. Specifically significant are the results of spatial resolution obtained using this mixture in and out of a high magnetic field. Additionally, the construction of the drift chamber and essential ionization theory of gases within a chamber is discussed.

CHAPTER II

CONSTRUCTION OF THE DRIFT CHAMBER

General

The drift chamber used for this experiment at Brookhaven National Laboratory was constructed at the Continuous Electron Beam Accelerator Facility (CEBAF), Newport News, Virginia. It is a prototype drift chamber similar in design to the tracking chambers proposed for the CEBAF Large Acceptance Spectrometer (CLAS).

The Chamber Body

The drift chamber, shown in figure 2, is wedge shaped and resembles a trapezoid with equally angled ends. The sense and field wires run parallel to the front and back faces of the chamber.

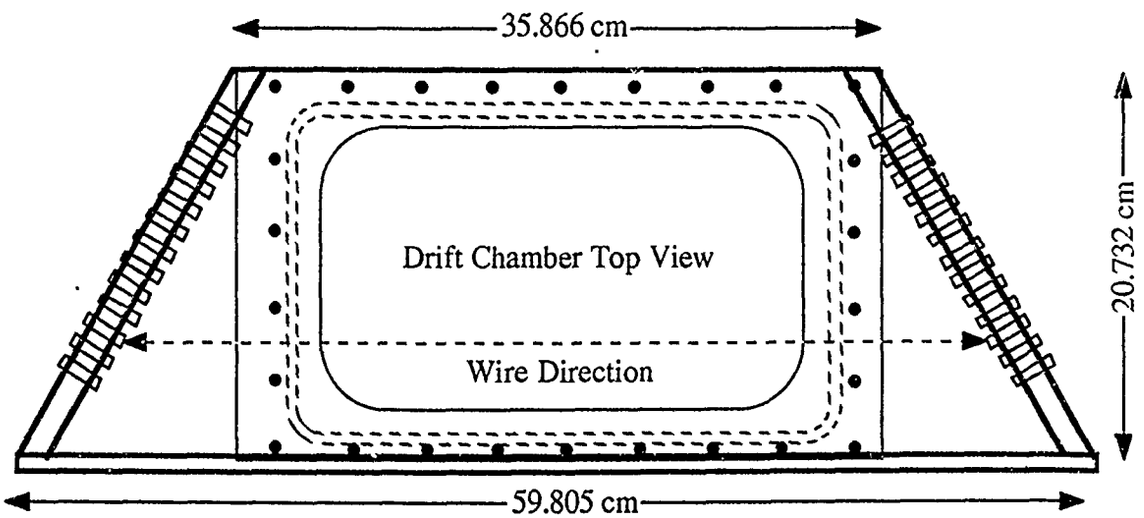

Fig. 2. Dimensions of the Drift Chamber [Ref. 5].

The chamber body [Ref. 6] is made of one-half inch and one-quarter inch aluminum plate with the dimensions shown in figure 2. The angle of the inclined ends is sixty degrees up from the interior horizontal bottom edge as shown in the figure. This tilting of the end plates minimizes the error in the actual position of the field and sense wires. With the crimp pins 200 microns in diameter and a sense wire of 20 microns in diameter, the error of actual wire position can vary as much as ten percent. Hence, with the inclined end plates and the tension on the wires, the position of the wire becomes fixed to the "bottom" edge of the crimp pin as opposed to any random position within the crimp pin. On the front, back and sides are window plates which are made of aluminized nylon. For observation within the chamber, clear mylar is used as windows. To prevent gas chamber leaks and unwanted air or other impurities entering the chamber, each plate or piece of the chamber is grooved for an O-ring.

The end plates of the drift chamber are drilled with two hundred and twenty four 0.1875 (3/16") inch holes each and one gas flow hole of 0.25 (1/4") inch. The 3/16 inch holes are arranged in a hexagonal arrangement as shown in figure 3. The dimensions of each plate are given in the figure.

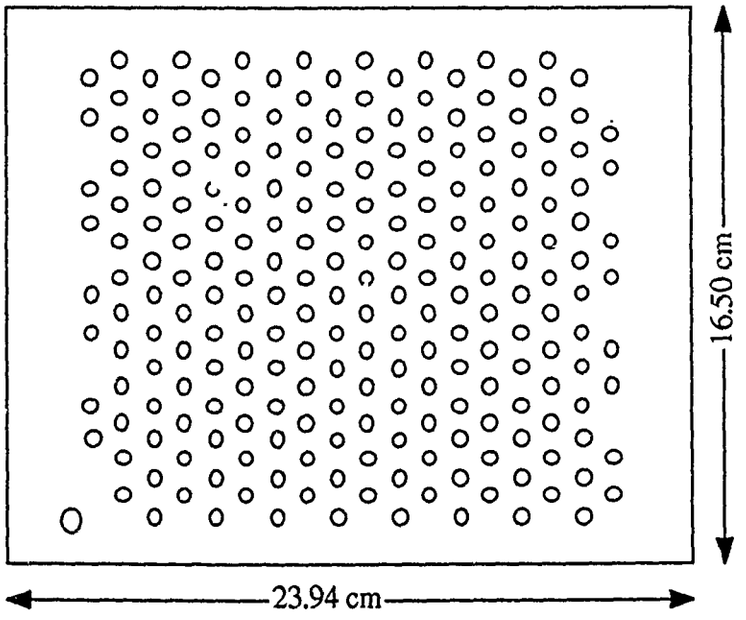

Fig. 3. Drift chamber End Plates [Ref 7].

Inserted into each of these holes on both plates were injection-molded plastic feed-throughs. These feed-throughs are sealed into place using low out gassing epoxy (Shell Epon 826:Versamid 140). It was found that these feed-throughs are sensitive to humidity and hence become slightly conductive. To overcome this, dry nitrogen was passed over the externally exposed feed-throughs during operation of the chamber.

Wiring the Drift Chamber

After a thorough cleaning of the chamber with ethanol and de-ionized water, the chamber was prepared for the stringing of the sense and field wires. The wires that are used in the chamber are 20 micron gold plated tungsten wire for the sense wires and 140 micron gold plated aluminum wires for the field wires.

The chamber was strung in a clean room to minimize dust and other particles from entering the chamber. To facilitate the wiring process, the chamber was fixed in an upright position such that the endplates were directed towards the ceiling and floor respectively. The pattern for stringing the field and sense wires is shown in figure 4.

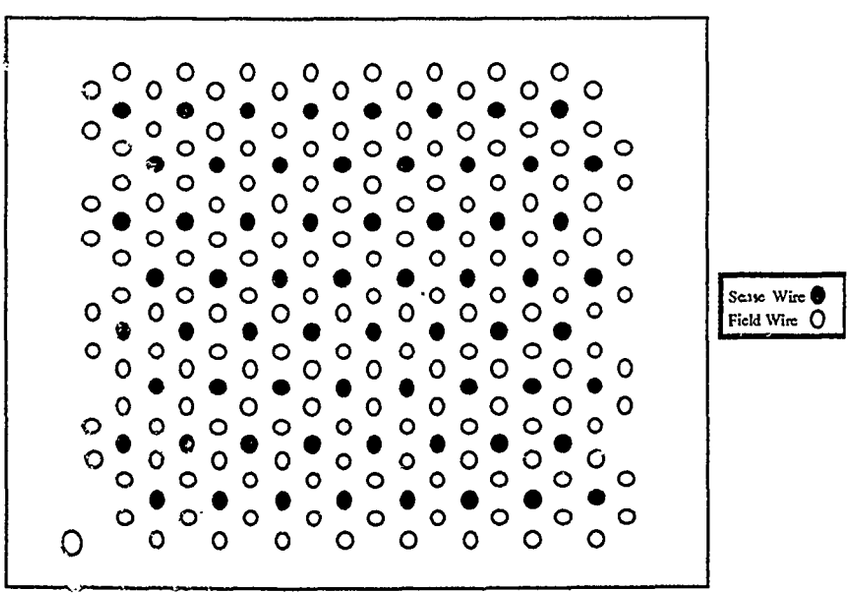

Fig. 4. Field and Sense Wire Pattern for Drift Chamber.

To string each wire, the following procedure was used. A wire was first passed through the 200 micron opening of a gold plated oxygen free hydrogenated copper crimp pin and then attached to a long sturdy sewing needle. Next, the crimp pin was seated into the feed-through. Using any manner convenient and ensuring the wire was kept clean, the wire was slowly rolled off its spool (while preventing any kinking or twisting of the wire) allowing the needle and wire to pass through the length of the chamber. With a magnetized pin inserted through the bottom the feed-through (corresponding to the same position as the top feed-through), the sewing needle was secured and brought through the second feed-through. Next, the top crimp pin was crimped using a machined crimping tool which was set to 0.038 inches for a flat crimp. This crimp secured the wire in the top crimp pin and allowed for tensioning of the wire. From the bottom of the chamber, the wire was passed through a second crimp pin which was then seated into its feed-through. Mass weights of 27 grams and 134 grams for the sense and field wire respectively were suspended from the wire to apply proper tension on the wire. Finally, the bottom crimp pin was crimped and the wire cut flush to the crimp pin. To prevent any slippage of the wire, a small drop of "Wonder Bond" or "Crazy Glue" was applied to the tip of the crimp pin.

After the chamber was completely strung, an electronic continuity check was performed to ensure that no wires were crossed in the wiring process. Any wires that were crossed required the replacement of both wires. The wires were replaced using the same wiring technique described above.

Chamber Electronics

To efficiently transmit the signals detected by the sense wires out to the data acquisition system, a simple yet elegant system of circuit boards was developed at CEBAF. The translator board, a printed circuit board with forty-two 0.1μF capacitors,

provided the means of bringing each sense wire signal into an array of twelve for easy transmission by means of a 24-pin double row card connector. The translator board was comprised of four card connectors.

Attached to the translator board were three pre-amplifier cards. Each card is capable of amplifying up to 12 sense wire signals. The heart of the pre-amplifier card is the MB43458 Fujitsu Quad Preamplifier chip. As implied by the chip name, each Fujitsu chip governs four signals. With three of these chips per pre-amplifier board, each board amplified 12 different signals. Figure 5 shows the translator board and one of the the pre amplifier cards attached to it.

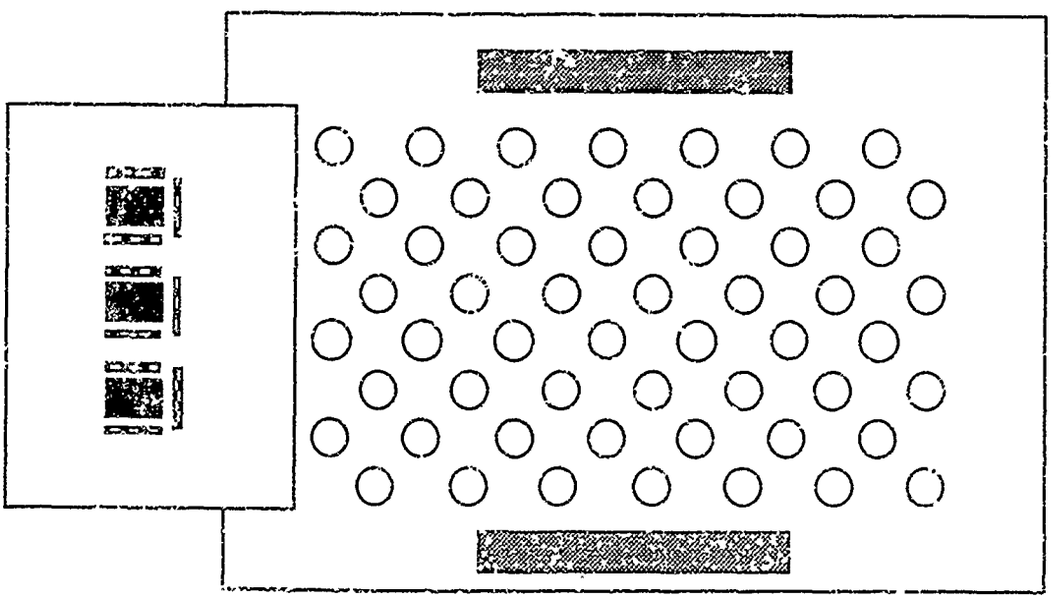

Fig 5. Translator and Pre-amplifier Board Assembly.

CHAPTER III

EXPERIMENTAL SET-UP

General

The experimental set-up at Brookhaven National Laboratory consisted of three major systems -- the gas flow system, the drift chamber, and the data acquisition system A pictorial overview of the set-up is shown in figure 6.

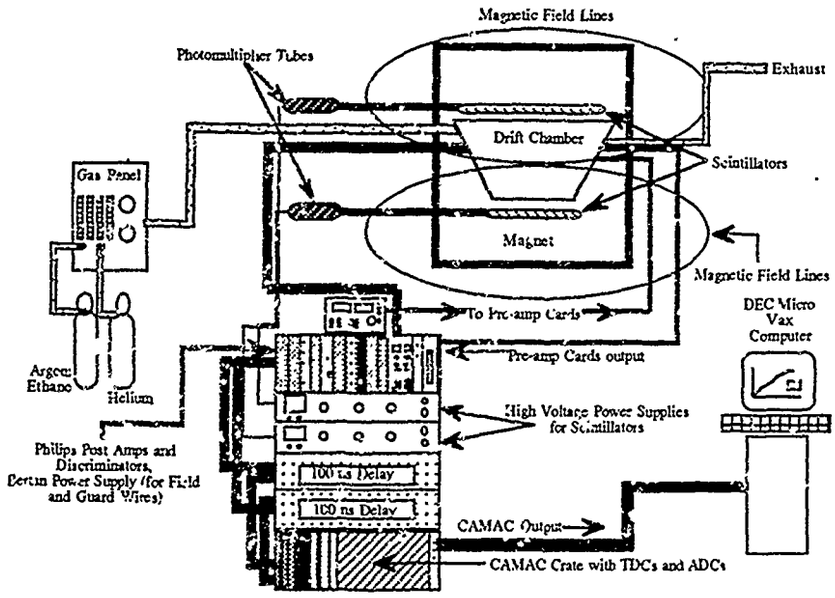

Fig. 6. Experiment Set-up

The Gas Flow System

The gas flow system, constructed at the University of New Hampshire, provided flow and mixture control of the gases used in the chamber. Essential elements of the system are the gas cylinders of 99.99% pure helium and 50:50 (by volume) argon:ethane; the Matheson flow meters for each gas; and the magnehelic gas

pressure meter. The gases entered the gas flow system from their respective cylinders into the flow meters. From the flow meters, the gases were mixed in a stainless steel manifold and then flowed through fifty feet of 0.25 inch nylon tubing. Beyond the chamber, the gases flowed through 0.25 inch "Nyflo" tubing through a back pressure jar filled with Corning Vacuum Pump Oil and out of the building.

The final component of the gas flow system was the nitrogen flow system around the gas chamber. This system was necessary to protect the feed-throughs from drawing humidity from the atmosphere. If the feed-throughs absorbed any moisture on the surface, they became conductive enough to draw current. This caused the power supply for the wires to trip its circuit breaker.

The Drift Chamber - Magnet System

The drift chamber was set inside the large 48D48 magnet with the wires in a horizontal position parallel to the floor. Positioned approximately two inches over the chamber was a "fat" scintillator (12" long X 6" wide X 2" thick). Positioned underneath the chamber, was a "thin" scintillator (12" long X 12" wide X 0.5" thick). The scintillators were attached to six foot long Lucite lightguides which were connected to an Amperex XP2269B photomultiplier tube. The high voltage power supplies for the photomultiplier tubes were set at 1850 and 1952 volts respectively. The signal pulse from each scintillator entered into a Phillips Model 715 Five Channel Timing Discriminator. The top scintillator discriminator was set at 25 mV and the bottom discriminator was set at 101 mV. Next, the signals came off the discriminators into separate sections of the Phillips Model 755 Quad Four Logic Unit that was set on coincidence 4. The signals from the logic unit were sent to the Phillips Model 792 Dual Delay Module, which was set at a 4 ns delay, and to both the TDC common start and ADC gate inputs.

The large 48D48 magnet is a dipole magnet capable of generating fields of up to 1.5 Tesla. The field lines of the magnet are oriented such that they are parallel to the chamber wires in the middle of the magnet. Control of the magnet field strength was maintained by setting field point voltages for the magnet's direct current power supply.

Electronics

The electronics of the system provided the necessary voltage to the pre-amplifier cards, the field and guard wires on the chamber, and to the photomultiplier tubes of the scintillators. Additionally, the electronics conducted the necessary signal amplification discrimination and delay for collection into the data acquisition system.

The field wires of the drift chamber were connected to a Bertan Model 375N High Voltage Supply. The A channel provided the voltage for the guard wires while the B channel supplied the voltages for the field wires. Additionally, the circuit breaker of the power supply was set to trip if more than 100 μA of current leakage was detected. Together with a Fluke 77 Digital Multimeter, the desired voltage for the field and guard wires could easily be set.

The Leader LPS-151 DC Tracking Power Supply provided the voltage and current to the pre-amplifier cards. These were set at 15 volts and 360 mA respectively and maintained throughout the experiment. Pre-amplifier card #1 was connected to sense wires numbered 1,2,3,7,8,9,13,14,15,19,20, and 21. Pre-amplifier card #2 instrumented wires numbered 25,26,27,28,29,30,31,32,33,34,35,36 with the last four wires terminated using a 10MΩ resistor and pre-amplifier card #3 instrumented sense wires numbered 4,5,6,10,11,12,16,17,18,22,23,24.

Using one RG-178 LEMO cable per channel (32 channels instrumented), the signals from the pre-amplifier cards were brought into a Phillips Model 778 Sixteen Channel Post Amplifier. Next, with a six inch LEMO connector, the signals were brought into a Phillips Model 706 Sixteen Channel Discriminator. The Phillips 706s

were set to discriminate signals less than 20 mV. From the discriminator, the signals were delayed 100 ns.

After the delay, the signals entered the CAMAC crate and into one of four LeCroy 2228 TDCs (Time to Digital Converter). From the TDCs the signals entered the LeCroy 2249 ADC (Analog to Digital Converter) Gates. Thus together with the timing signal sent from the scintillators and the signal pulse from any sense wire, the drift time of the electrons was determined.

Data Acquisition System

The final section of the hardware for the experiment setup was the data acquisition system. This consisted of a Digital Equipment Corporation Microvax computer. Data files from the TDCs and ADCs were read onto the system's hard disk and stored for each run. Backup copies of the runs were made on the computer system at Brookhaven BNLDAG.

The software program to analyze the data was written at CEBAF. It was an elaborate program that reconstructed the track of a cosmic ray after it traversed the drift chamber. The types of data stored included scintillator times produced by a trigger; which sense wires recorded at hit; the time off the TDC for each sense wire hit; and the total number of hits. With the data, the program was able to calculate how far from each sense wire the ionized electrons were located. With several sense wires signalling, a track could be reconstructed.

Many parameters could be changed using the track program. Items of interest were the zero set time (T0) of the Time to Digital Converters (TDCs), the excluded layer (a user selected row of sense wires to collect individual wire statistics), and the velocity function (parameters on which the program calculated the track). A sample of the statistics output is shown in figure 7, and in figure 8 is an example of a reconstructed track.

TRACK SYSTEM STATUS RUN# 99

15:21:26 26-NOV-90

PARAMETERS:

	GUARD	SENSE	FIELD
Voltage(v):			2000.0
Discriminator(mv):			20.00
Cell Border(cm):			0.06
Mean TDC Cut[t0](ns):			13.00
Time Scale(ns):			600.0
Excluded Layer:			3
Excluded wires:			33 34 35 36 0

Relative TDC Offsets[t00](ns):

Channel 1 - 6:	0.00	0.00	0.00	0.00	0.00	0.00
Channel 7 - 12:	0.00	0.00	0.75	0.75	0.75	0.75
Channel 13 - 18:	0.75	0.75	0.75	0.75	-0.25	-0.25
Channel 19 - 24:	-0.25	-0.25	-0.25	-0.25	-0.25	-0.25
Channel 25 - 30:	3.50	3.50	3.50	3.50	3.50	3.50
Channel 31 - 36:	3.50	3.50	0.00	0.00	0.00	0.00

v0 : 2000.00

thmin : 0.0000 thmax : 0.5236

timev : 0.000 140.000 200.000 215.000 320.000
360.000 400.000 480.000 520.000

xv : -0.040 0.379 0.518 0.549 0.711 0.768 0.811 0.876 0.891
-0.040 0.379 0.518 0.549 0.711 0.800 0.850 0.922 0.930

ANALYSIS RESULTS:

Number of Triggers:	1062
Total tracks through layer:(T)	358
Tracks through cells which did not signal:(N)	18
Percentage: (N/T)	5.03%
Cells signalling which did not contain tracks:(M)	3
Percentage: (M/T)	0.87%
Number of inefficiencies with maxtim < t < timeout:	0
Number of inefficiencies with track near border (<.060 cm):	17
Number of tracks through layer:(LT)	235
Number of times layer fired:(LN)	235
Percentage: (LN/LT)	100.00%
Total cells signalling:	343
Number of inefficiencies with track near cell (<.060 cm):	0
The average residual (cm):	-0.2393E-02
10-bin rms value (cm):	0.2321E-01
The average residual of excluded layer(cm):	0.2672E-01
10-bin rms value of excluded layer(cm):	0.2425E-01

COMMENTS:

First run at B=0 for (63:18.5:18.5) Helium:Argon:Ethane

Fig. 7. Sample of Run Data Sheet Output

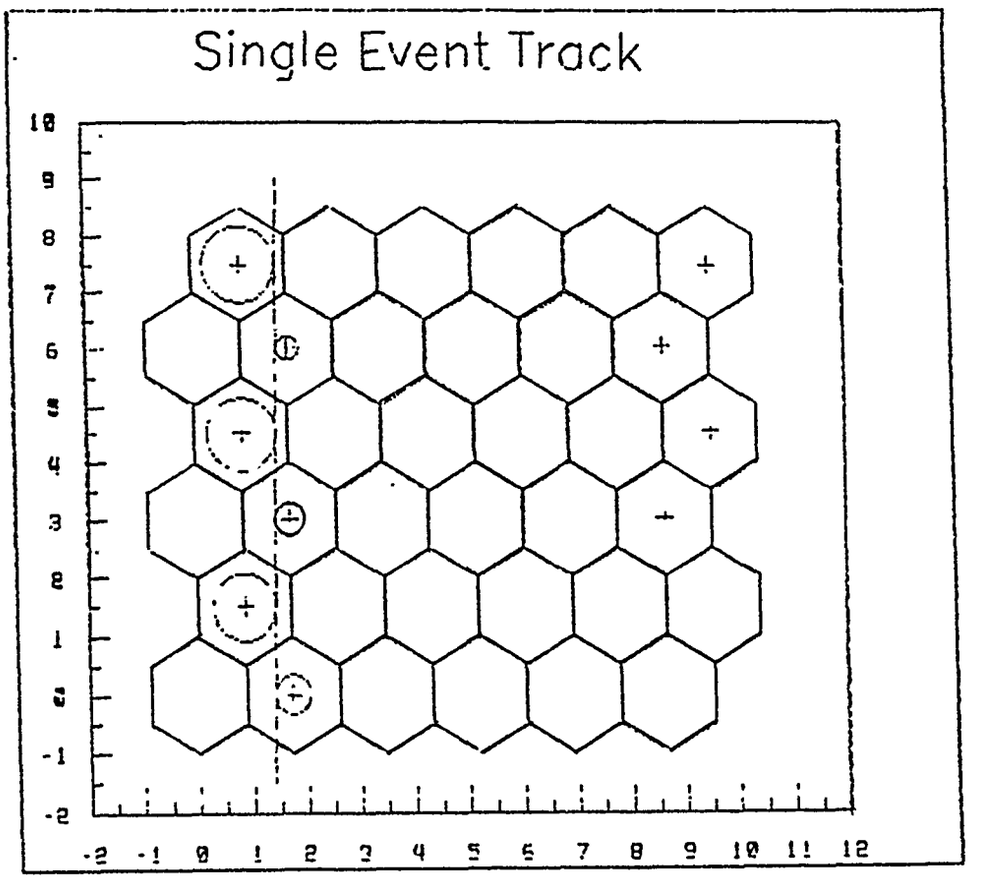

Fig. 8. Fit of a Cosmic Ray Track.

CHAPTER IV

THEORY OF OPERATION

Diffusion of Electrons and Ions in Gases [Ref. 1, 8, 9, 10]

For drift chambers, an understanding of the motion of electrons and ions in gases is extremely meaningful. It is the motion of these particles which influence the operating characteristics of the chamber. The basic theory which describes this motion is the classical theory of gases. The two most important phenomena are the diffusion and drift of electrons and ions in an electric field [Ref. 1, 2].

A fast charged particle moving through a gas medium interacts in many ways. With respect to the drift chamber, the electromagnetic interaction is the most important because it is this process that is used for signal detection. With the passage of a particle, a finite number of primary ionizing collisions occur which free electron-ion pairs in the medium. Ejected electrons having energy greater than that of the ionization potential of the medium may produce a second ion pair. The sum of these two contributions is total ionization. The total number of ion pairs [Ref. 1] is given by

$$n_T = \frac{\Delta E}{W_i} \tag{4.1}$$

where ΔE is the total energy loss in the gas medium considered, and W_i is the effective average energy to produce one electron-ion pair. Table 1 [Ref. 1, 11, 12] provides pertinent data for gases of interest, where W_i is the average energy to produce one ion pair, I_0 is the ionization potential in electron volts, and n_t and n_p are the total number of ion pairs and primary number of ion pairs respectively.

Gas	Z	A	ρ (gm/cm^3)	dE/dx (keV/cm)	dE/dx (MeV/gcm^{-2})	I_o (ev)	W_i	n_p (i.p./cm)	n_t (i.p./cm)
He	2	4	1.66E-04	0.32	1.94	24.6	41	5.9	7.8
Ar	18	40	1.66E-03	2.44	1.47	15.8	26	29.4	94
Ethane	18	30	1.25E-03			11.8	24.6		

Table 1. Properties of Gases used in the LAS Drift Chamber.

These electrons and ions quickly lose their energy through multiple collisions with the gas molecules. Hence these charged particles come into thermal equilibrium with the gas and eventually reunite. The drift velocity of these particles is given as [Ref. 2]

$$v = \sqrt{\frac{8kT}{\pi m}} \tag{4.2}$$

where k is Boltzman's constant, T the temperature, and m the mass of the particle. Under normal conditions, these charged particles move about with a Maxwellian energy distribution with a most probable value of $\frac{3}{2}kT$ which is approximately 0.04 eV at room temperature. The Maxwellian distribution of kinetic energy ε at a temperature T is described as a function of ε as

$$F(\varepsilon) = C\sqrt{\varepsilon}\, e^{-(\varepsilon/kT)}\,. \tag{4.3}$$

Recognizing the inverse relationship of velocity to the particle mass, it is obvious that electrons move with a much greater velocity than that of ions. Under normal conditions, the drift velocities of electrons are roughly 1000 times greater than those of positive ions [Ref. 3].

After a time t, the distribution of the charged particles diffusing through multiple collisions is given by a Gaussian distribution [Ref. 1]

$$\frac{dN}{N_0} = \frac{1}{\sqrt{(4\pi Dt)}} \exp\left(-\frac{x^2}{4Dt}\right)dx \tag{4.4}$$

where dN/N_0 is the fraction of charged particles found in the element dx at a distance x from its point of creation and D is the diffusion coefficient. The root mean square (rms) spread of the distribution, or in other words its standard deviation, in any one direction, say x, is given by

$$\sigma_x = \sqrt{2Dt} \tag{4.5}$$

For a volume diffusion, the spherical dispersion is given for r in a radial distance as

$$\sigma_r = \sqrt{6Dt}\,. \tag{4.6}$$

The diffusion coefficient is proportional to velocity and the mean free path of the electron or ion. D is usually given as

$$D = \frac{1}{3} v\lambda. \tag{4.7}$$

For a classical ideal gas [Ref. 2] , the mean free path for an electron or ion in a gas is a function of temperature T, pressure P, and the total cross-section for a collision with a gas molecule. The mean free path is given as

$$\lambda = \frac{2}{3\sqrt{\pi}} \frac{kT}{\sigma_0 P}. \tag{4.8}$$

Substituting the formula for the mean free path (4.6) into (4.5), an explicit expression for the diffusion coefficient is obtained,

$$D = \frac{2}{3\sqrt{\pi}} \frac{1}{P\,\sigma_0} \sqrt{\frac{(kT)^3}{m}}. \qquad (4.9)$$

From equation (4.7), the dependence of various parameters of the gas for its diffusion becomes clear.

Drift and Mobility of Electrons and Ions

Under the influence of an electric field E, the electrons and ions gain kinetic energy and accelerate towards the anode and cathode respectively in the direction of the field. This acceleration is interrupted by the collisions with other molecules and atoms thereby limiting the maximum average velocity which can be obtained by the charge. This average velocity is the drift velocity of the charge. As expected, the drift speeds of electrons are much higher than those of ions. Drawing on kinetic theory, the mobility, μ, of an ion or electron is given as

$$\mu = \frac{w}{E} \qquad (4.10)$$

where w is the drift velocity and E is the electric field strength. For positive ions but not for electrons, it is discovered that drift velocity is linearly proportional to the reduced field E/P, where P is the gas pressure, over a wide range up to large fields. Therefore, for positive ions at constant pressure, mobility is constant: for a fixed electric field, it varies inversely to gas pressure.

Using the notion of an ideal gas, an expression for the relationship between mobility, μ, and the diffusion coefficient, D, for charged particles in thermal equilibrium is given by the Einstein relation

$$\frac{D}{\mu} = \frac{kT}{e}. \tag{4.11}$$

For a mixture of n various gases, the mobility μ_i of the ion belonging to the ith gas component is given by

$$\frac{1}{\mu_i} = \sum_{k=1}^{n} \frac{c_k}{\mu_{ik}} \tag{4.12}$$

where c_k is the concentration by volume of the kth gas and μ_{ik} is the mobility of the ion of the ith component in the kth gas.

A significant aspect to consider for a mixture of gases is that if several kinds of ions are present, then the gases with the higher ionization potential become neutralized after 10^2 - 10^3 collisions by removing electrons from atoms with lower ionization potentials [Ref. 8]. For example, helium, with the highest first ionization potential of all the gases, becomes neutralized after several hundred to several thousand collisions. Its effect in the gas mixture is that of elastic collisions with the charged particles and other molecules. One could say that it acts like a "glass ball" or a pressurized vacuum within the gas volume.

Except for low electric fields, the mobility of electrons is not constant. Because of their small mass, electrons increase their energy between collisions with gas molecules under the influence of an electric field. Under the influence of an electric field **E**, the electrons move in a total motion in the direction of the field with a drift velocity *w* [Ref. 9] :

$$w = \frac{eE/\lambda}{m\ v} = \frac{eE\tau}{m} \tag{4.13}$$

where v is the velocity of the electron, λ the mean free path of the electron, and τ, in general a function of E, the average collision time. Ideally, in the case in which electrons do not appreciably modify their energy with increasing E, the mean collision time τ is treated as a constant value. As a result, the drift velocity increases linearly with the field. Hence the following relationship holds:

$$eE\frac{D}{w} = kT \tag{4.14}$$

Often kT is expressed as the characteristic energy ε_k; as observed in equation (4.14), ε_k is a function of E and is dependent on drift velocity and diffusion. Developing an expression for the drift velocity, *w*, after rearranging the above equation and substituting it into the Gaussian distribution, the expression for the thermal limit to electron diffusion width is obtained.

$$\sigma_x = \sqrt{\frac{2kTx}{eE}}. \tag{4.15}$$

Using the expression for ε_k, and incorporating the reduced field E/P, a quantity that can be measured, the diffusion width [Ref. 9] can be stated as:

$$\sigma_x = \sqrt{\frac{2\ \varepsilon_k x}{eE}} = \sqrt{\frac{2\ \varepsilon_k}{eE/P}}\sqrt{\frac{x}{P}} \tag{4.16}$$

In this expression, it is apparent that electron diffusion has an inverse square root dependence on pressure at a given value of E/P.

Recent rigorous studies have been made regarding electron drift in gases, notably Palladino and Sadoulet [Ref. 10] and Schultz and Gresser [Ref. 13].

Although the details are beyond the scope of this thesis, the main points are summarized [Ref. 9,10]. First an electron density distribution function is introduced using the six dimensional phase space at time t of position and velocity, $f(\mathrm{v},\mathrm{r},t)$. This function is expressed in a differential form and it describes both the electron swarm density and energy conservation.

$$\frac{\partial f}{\partial t} + \frac{\partial f \partial \mathrm{r}}{\partial \mathrm{r} \partial t} + \frac{\partial f \partial \mathrm{v}}{\partial \mathrm{v} \partial t} - \left.\frac{\partial f}{\partial t}\right|_{\text{via collisions}} = 0 \qquad (4.17)$$

This expression is next expressed in terms of the applied electric field E (radiating outwardly from the sense wires in the r direction) , the electron energy $\varepsilon = \frac{1}{2}\mathrm{m}\mathrm{v}^2$, the momentum transfer mean free path $\lambda_e(\varepsilon)$, the mean free path $\lambda_h(\varepsilon)$ for the *h*th excitation level of energy. In the stationary case of the classical theory of electrons for the particular case when the magnetic field is perpendicular to the electric field, such as when the **B** field lines are parallel to the sense and field wires, there is no *x* and *t* dependence; furthermore, symmetry arguments restrict the dependence to ε and $\cos\theta$ where θ is the angle of flight with respect to the x axis. Hence the distribution function takes the normalized form

$$\int_0^{t_{\max}} F(\varepsilon, \cos\theta)\, d\varepsilon \, \frac{d\cos\theta}{2} = 1 \,. \qquad (4.18)$$

To solve this equation, $F(\varepsilon,\cos\theta)$ is expanded in Legendre polynomials: keeping only the first two terms, $F(\varepsilon,\cos\theta) = F_0(\varepsilon) + F_1(\varepsilon)\cos\theta + ...$, two coupled differential equations are obtained. These are [Ref. 9],

$$eE\frac{\partial(vF_0)}{\partial\varepsilon} - \frac{2eE}{mv}F_0 + \left(1 + \frac{e^2H^2\lambda^2_e}{2m\varepsilon}\right)\frac{vF_1}{\lambda_e} = 0 \quad \text{and} \tag{4.19}$$

$$\frac{eE}{3}\frac{\partial(vF_1)}{\partial\varepsilon}\left(\frac{evF_0}{\lambda_\varepsilon}\right) - \frac{2m}{M}\frac{\partial}{\partial\varepsilon}\left(\frac{evF_0}{\lambda_e}\right) - \sum_h\left(\frac{\sqrt{2(\varepsilon+\varepsilon_h)/m}}{\lambda_h(\varepsilon+\varepsilon_h)}F_0(\varepsilon+\varepsilon_h) - \sqrt{\frac{2\varepsilon}{m}}\frac{F_0}{\lambda_h}\right) = 0.$$

The summation in equation (4.19) refers to the effect of the inelastic cross sections appearing at the energy ε_h with the electron mean free path λ_h; λ_e is the elastic collision mean free path. The variables λ_h and λ_e are functions of ε and can be obtained from the related cross sections from the expression

$$\lambda(\varepsilon) = \frac{1}{N\sigma(\varepsilon)} \tag{4.20}$$

where N is the number of molecules per unit volume. At a particular temperature T and pressure P, N is given by

$$N = N_0\frac{P}{760}\frac{273}{T} \text{ molecules } m^{-3} \text{ where } N_0 = 2.69 \times 10^{25}. \tag{4.21}$$

The differential equations in (4.19) can be computed using numerical analysis or solved by making some broad approximations for the quantities involved. Therefore, solutions of these equations allows $F_0(\varepsilon)$ and $F_1(\varepsilon)$ to be derived thereby providing the following expressions for drift velocity and diffusion coefficient:

(a) the drift velocity in the direction of E:

$$w_{\parallel} = -\frac{2}{3}\frac{eE}{m}\int\frac{\varepsilon\lambda_e[\partial(F_0/v)/\partial\varepsilon]}{1 + (e^2H^2\lambda_e^2/2me)}\,d\varepsilon \tag{4.22}$$

(b) the drift velocity in the direction perpendicular to E and H:

$$w_{\perp} = \frac{eH^2}{3m} \int \frac{\lambda_e^2 v[\partial(F_0/v)/\partial\varepsilon]}{1 + (e^2H^2\lambda_e^2/2me)} d\varepsilon . \tag{4.23}$$

(c) the transverse (or symmetric) diffusion coefficient:

$$D_H = \frac{1}{3} \int \frac{\lambda_e v F_0(\varepsilon)}{1 + (e^2H^2\lambda_e^2/2me)} d\varepsilon . \tag{4.24}$$

Making a broad assumption [Ref. 1], such as only a small amount of electrons gain enough energy to experience ionizing collisions, the energy distribution can be expressed as follows:

$$F_0(\varepsilon) = C\sqrt{\varepsilon}\, \exp\left(-\int \frac{3\Lambda(\varepsilon)\varepsilon}{[eE\lambda_e]^2 + 3\Lambda(\varepsilon)[1+(e^2H^2\lambda^2_e/2m\varepsilon)]} d\varepsilon \right). \tag{4.25}$$

$\Lambda(\varepsilon)$ is the fraction of energy lost on impact due to absorption in the rotational and vibrational modes, or in other words, its inelasticity. It is determined as

$$\Lambda(\varepsilon) = \frac{2m}{M} + \sum_h \frac{\varepsilon_h}{\varepsilon} \frac{\lambda_e}{\lambda_h} = \frac{2m}{M} + \sum_h \frac{\varepsilon_h}{\varepsilon} \frac{\sigma_h}{\sigma_e} \tag{4.26}$$

with m and M the masses of the electron and gas molecules respectively. The terms $\sigma_e(\varepsilon)$ and $\sigma_h(\varepsilon)$ are the elastic (momentum transfer) and inelastic cross-sections, and ε_h is the excitation energy of state h. The variable $\sigma(\varepsilon)$ [Ref. 1] is the cross section deduced from the Ramsauer curve of the gas under consideration. If the cross-sections for elastic and inelastic scattering are known, then $F(\varepsilon)$ can be computed.

Subsequently, the drift velocity and diffusion coefficient are given as follows:

$$w(E) = -\frac{2}{3}\frac{eE}{m}\int \varepsilon\lambda(\varepsilon)\frac{\partial[F(\varepsilon)\, u^{-1}]}{\partial\varepsilon}\, d\varepsilon \tag{4.27}$$

and

$$D(E) = \int \frac{1}{3} u\lambda(\varepsilon) d\varepsilon \tag{4.28}$$

where $u = \sqrt{2\varepsilon/m}$ is the instantaneous velocity of electrons of energy ε.

For gas mixtures a simple substitution is made for equations (4.25 and 4.26). The cross-sections and energy losses are as follows [Ref. 9]:

$$\sigma_e(\varepsilon) = \sum_i p_i\sigma_i(\varepsilon) \quad \text{and} \quad \Lambda(\varepsilon) = \frac{1}{\sigma_e(\varepsilon)} \sum_i p_i\sigma_i(\varepsilon)\lambda_i(\varepsilon) \tag{4.29}$$

where p_i is the fraction of gas i in the mixture, $\lambda_i(\varepsilon)$ and $\sigma_i(\varepsilon)$ are, respectively, its elastic cross-section and energy loss as described in equation (4.26).

The conclusion of this statistical transport theory is that essentially two parameters characterize a gas mixture. First is the cross-section for elastic collisions $\sigma_e = \sigma_e(\varepsilon)$ which in turn is related to $\lambda_e(e)$ via equations (4.20) and (4.21). Second is the mean fraction of energy lost by an electron at the time of collision $\Lambda = \Lambda_e(\varepsilon)$ which is found through equation (4.23) after finding the excitation energy ε_h of the h^{th} level together with the cross-section σ_h of the type of collision involved in this excitation level [Ref 13].

Drift of Electrons in Magnetic Fields

A magnetic field alters the drift properties of a cluster of electrons. The Lorentz force acting on each moving charge changes both the small portion of motion between two collisions into circular trajectories and the energy distribution. The net effect of the magnetic field is a reduction in the drift velocity, especially at low electric fields. The electrons show a nonzero component of their drift velocity in the direction of E X B. The magnetic drift velocity, w_M [Ref. 10], is defined as

$$w_M = \frac{w_\perp}{w_\parallel}\frac{E}{B}. \tag{4.30}$$

Under conditions of constant collision time, that is $\frac{d\lambda}{dv} = \frac{\lambda}{v}$, the magnetic drift velocity can be expressed as

$$w_M = \frac{eE}{m}\frac{\lambda}{v} = w. \tag{4.31}$$

For calculation of the drift angle α, in which the electrons drift with respect to the electric field,

$$\tan\alpha = \frac{w_\perp}{w_\parallel} = \frac{Bw_M}{E}. \tag{4.32}$$

In the situation of travel in a constant electric and magnetic field, the electron swarm drifts along a straight line at an angle α_H with the field lines, and with a velocity $w_M \neq w$. The effect of a magnetic field **H** applied in a direction perpendicular to the electric field is given as follows:

$$w_M = \frac{w}{\sqrt{1+\omega^2\tau^2}}, \quad \text{with} \quad \omega = \frac{cH}{m} \quad \text{and} \quad \tan\alpha_H = \omega\tau. \tag{4.33}$$

If the expression, $\tau = \frac{2mw}{eE}$ is substituted in equation (4.33), the magnetic drift velocity

[Ref. 14, 15] can be expressed as a function of E, B, as

$$w(E,B) = \frac{w(E,B=0)}{\sqrt{1 + [2w(E, B=0)B/E]^2}}. \tag{4.34}$$

Avalanche Multiplication

As mentioned previously, after primary ionization some electrons have sufficient energy to produce additional ions. However, near the anode wires electrons gain sufficient energy between collisions from the electric field to ionize additional gas molecules [Ref. 16]. The electrons produced from this process can also gain energy from the field and ionize more molecules and so forth. This cascading process is the formation of an avalanche.

If the mean free path of a secondary electron collision is α, then $\frac{1}{\alpha}$ is the probability of an ionization per path length. This factor of α^{-1} is known as the Townsend coefficient [Ref. 3]. If there are η electrons, then for a path length dx, there will be $d\eta = \eta \alpha\, dx$ new electrons created. Integrating this first order equation gives the total number of electrons created in a path of length x.

$$\eta = \eta_0 e^{\alpha x}. \tag{4.35}$$

The multiplication factor for a gas then is the ratio

$$\frac{\eta}{\eta_0} = M = e^{\alpha x}. \tag{4.36}$$

Principles of Drift Chamber Operation

As mentioned earlier, the drift chamber used in this experiment incorporated a hex-cell design. The sense wire (ànode) is surrounded by six field (cathode) wires in a hexagonal design. A high negative voltage is maintained on the field wires while the sense wire is held at ground.

With the chamber filled with a gas mixture, for a cell consisting of surrounding long conducting parallel wires (approximating a cell), the electric field and potential is written as

$$E(r) = \frac{CV_0}{2\pi\varepsilon}\frac{1}{r} \qquad (4.37)$$

and

$$\Phi(r) = \frac{CV_0}{2\pi\varepsilon}\ln(\frac{r}{r_w}). \qquad (4.38)$$

The variable C, the capacitance, is given as

$$C = \frac{2\pi\varepsilon}{\ln(r_c/r_w)}. \qquad (4.39)$$

For these equations, r_w is the radius of the sense wire, r_c is the radius from the sense wire to the field wire, and r is the radius to a point inside the cell originating from the sense wire. V_0 is the potential on the field wire (V = 0 on the sense wire), ε the di-electric constant of the gas mixture, approximately 8.85 pF/m. With the radius of the cell much greater than that of the sense wire, the charge distribution on the wires is assumed uniform. Using equation (4.37) the charge on a wire from the potential of all the surrounding wires, not just the nearest neighbor, can be calculated. There is an important boundary condition here: the total charge of the system is zero. Hence, the chamber does not have infinite potential at infinity.

Figure 9 [Ref. 17] shows the electric field lines and isochrones of the potential for the hexagonal cell. Notice that close to the sense wire the potential is nearly circular, whereas near the outer edges the contours are hexagonal.

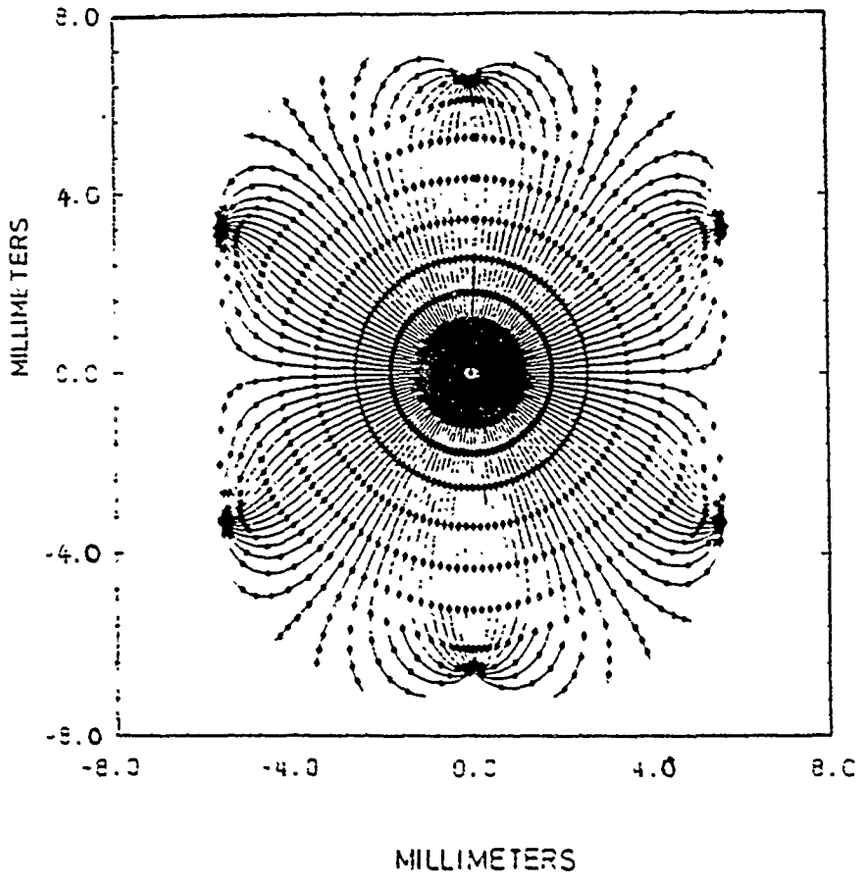

Figure 9. Electric Field Lines and Isochrones for the Hexagonal Cell.

CHAPTER V

THE EXPERIMENT

General

The data for this experiment were taken during testing of the prototype chamber (described in chapter two) at Brookhaven National Laboratory in September 1990. Although the goal of the primary research group, CEBAF, was to determine the operating characteristics of the chamber in a high magnetic field, a secondary opportunity was made manifest to examine the properties of novel gas mixtures for the chamber under the same stringent conditions.

After assembling the drift chamber system (described in chapter three) and completing the required diagnostics, the experiment required the completion of essentially three tasks. First was the calibration of the gas flow system; second was the determination of the efficiency curves, and finally the measurement. These processes are described in detail below.

Calibration of the Gas Flow System

The Matheson flow meters were calibrated using a 100 cc SKC flow calibration cylinder. At a given setting of the flow meter, the flux of the gas was measured and recorded. Calibration plots for argon:ethane and helium are provided in figures 10, 11 and 12. In all calibration runs, the glass ball reading of the gas flow meter was used.

Figure 10 is the initial calibration of (50:50) argon:ethane. It was the principle gas mixture used to test the drift chamber. For these initial runs of the experiment, the gas flow was set at 28.1 ml/min.

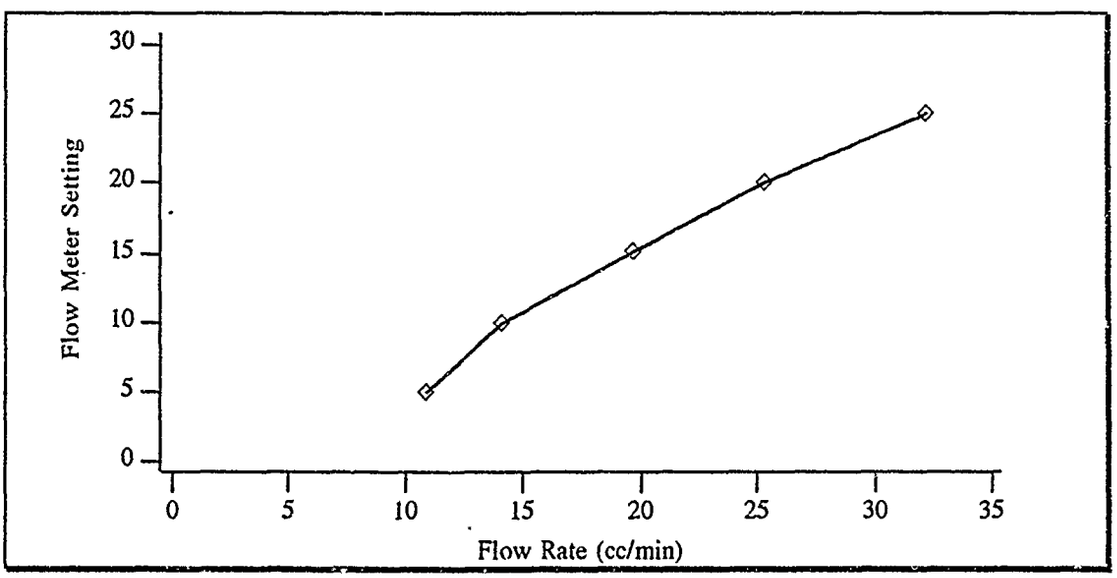

Fig. 10. Gas Flow Calibration of 50:50 Argon:Ethane.

Figure 11 is the helium calibration curve. Prior to calibration of the system, the chamber was flushed overnight with helium. To ensure that the gas was dominated by the helium, the gas flow rate was relatively high compared to that of argon:ethane. The flow rate for the helium was initially set at 56 (glass ball reading) or 89 cc/min.

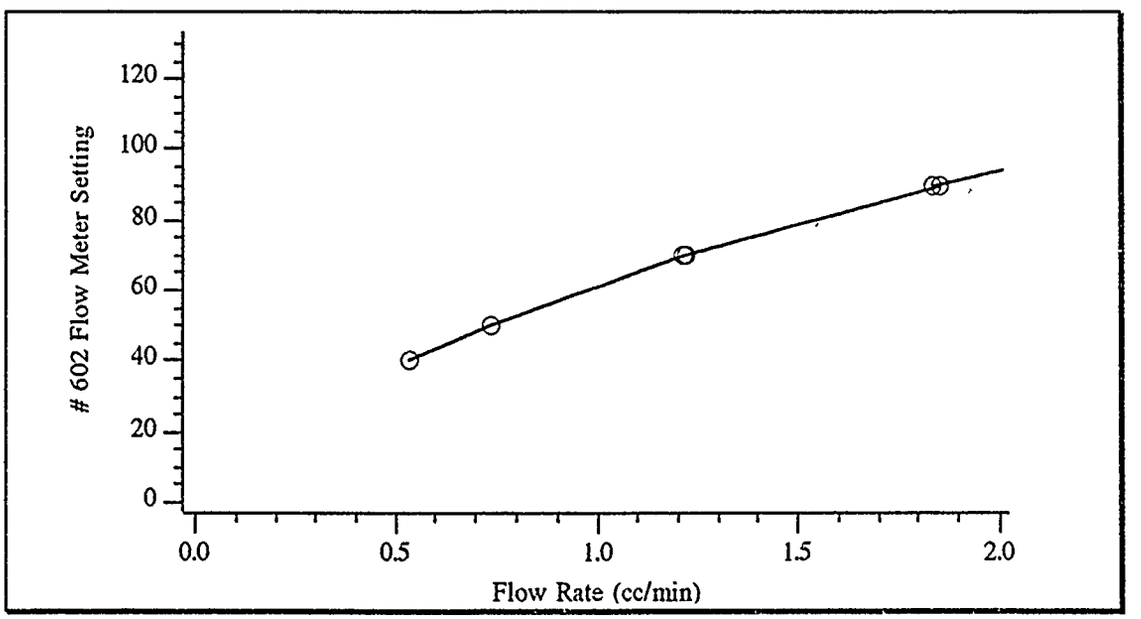

Fig. 11. Helium Gas Flow Calibration.

The calibration curve shown in figure 12 is argon:ethane using a second Matheson flow meter. Because the argon:ethane flowing into the chamber was to be at a much smaller flow rate than was previously measured, it was necessary to recalibrate the flow meter. In the figure, the top line is the Matheson 610A flow meters which were available for use. Although the curve parallels the 602 flow meter, the adjustment on the 610A was not reliable: subsequently, the 610A meters were not used. The argon:ethane flow rate was set at 35 (glass ball reading) for a flow rate of 52 cc/min.

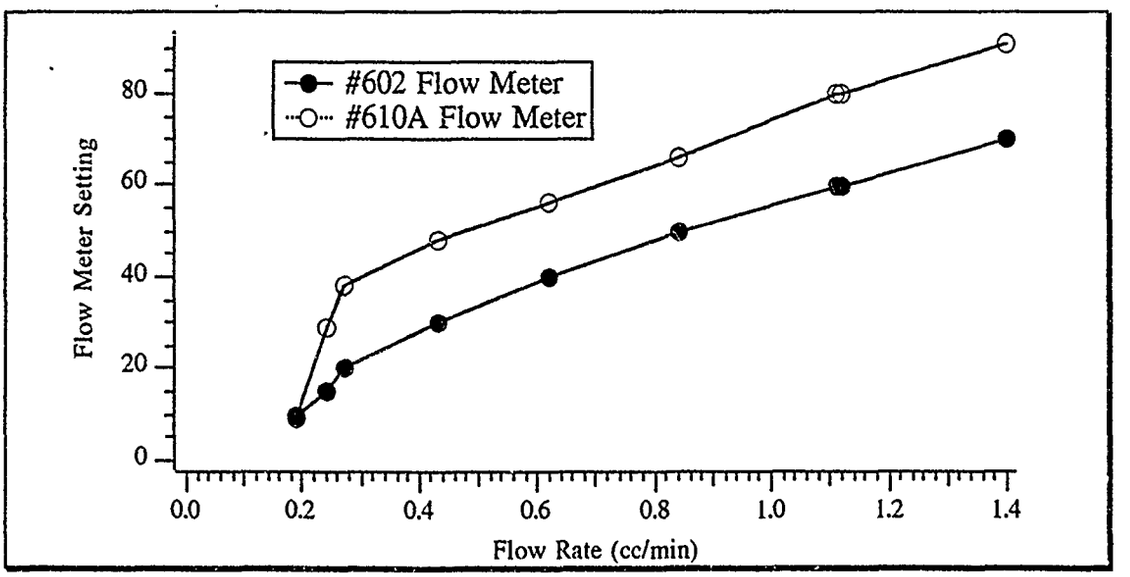

Fig. 12. Argon:Ethane Flow Meter Calibration for Slow Flow Rate.

Determination of the Efficiency Plateau

The efficiency plateau for the chamber is found by using the data of several experimental runs at various potentials on the field wires. At each voltage, the efficiency, (the number of tracks through a layer {LN} / the number of times the layer fired {LT}) is plotted. The voltage at which the efficiency is a maximum and provides the best accumulation of data is the desired voltage to collect data for the experiment itself.

The initial efficiency plot was completed at CEBAF prior to the experiment at Brookhaven so that initial conditions could be established. This plot is shown in figure 13.

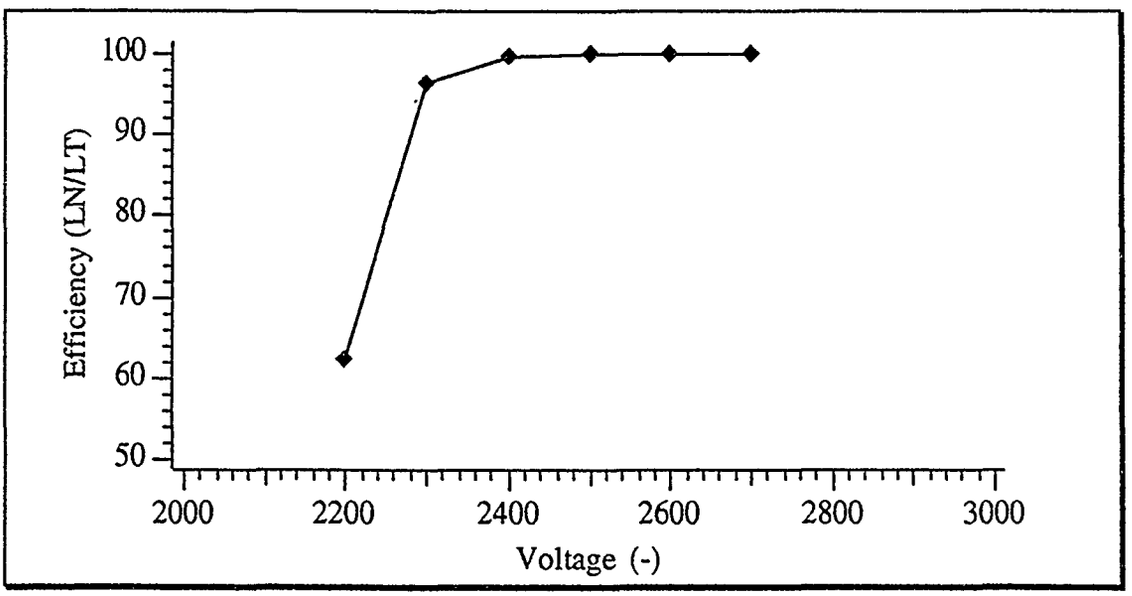

Fig. 13. Efficiency Plateau of Argon:Ethane vs. Voltage

The plot shown in figure 14 is the efficiency plateau for the helium:argon:ethane mixture at percentages of 63%:18.5%:18.5% respectively. The chamber was efficient at voltages above 2000 volts; however, at voltages greater than 2100 volts, the noise increased inside the chamber. Consequently, an operating voltage of 2000 volts was chosen for the experimental run.

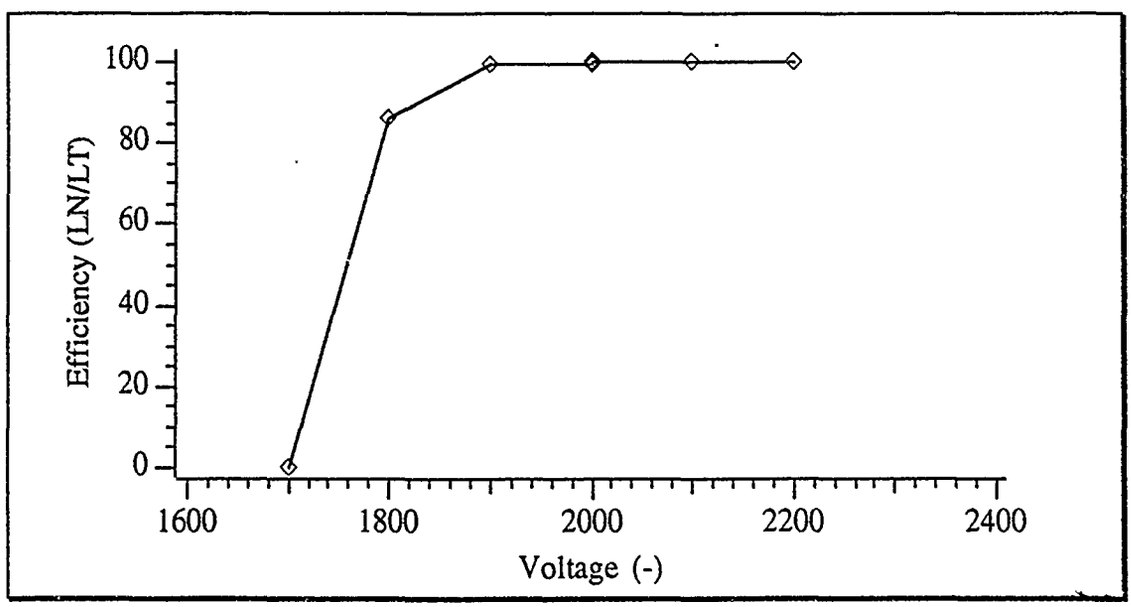

Fig. 14. Efficiency Plateau of Helium:Argon:Ethane vs. Voltage.

One additional efficiency plateau was made for a gas mixture that consisted of 81% helium, 9.5% argon and 9.5% ethane. This mixture proved to be too thin: it was extremely noisy and had a small working region as its plateau. This mixture was not usable; nevertheless, its efficiency plateau is shown in figure 15.

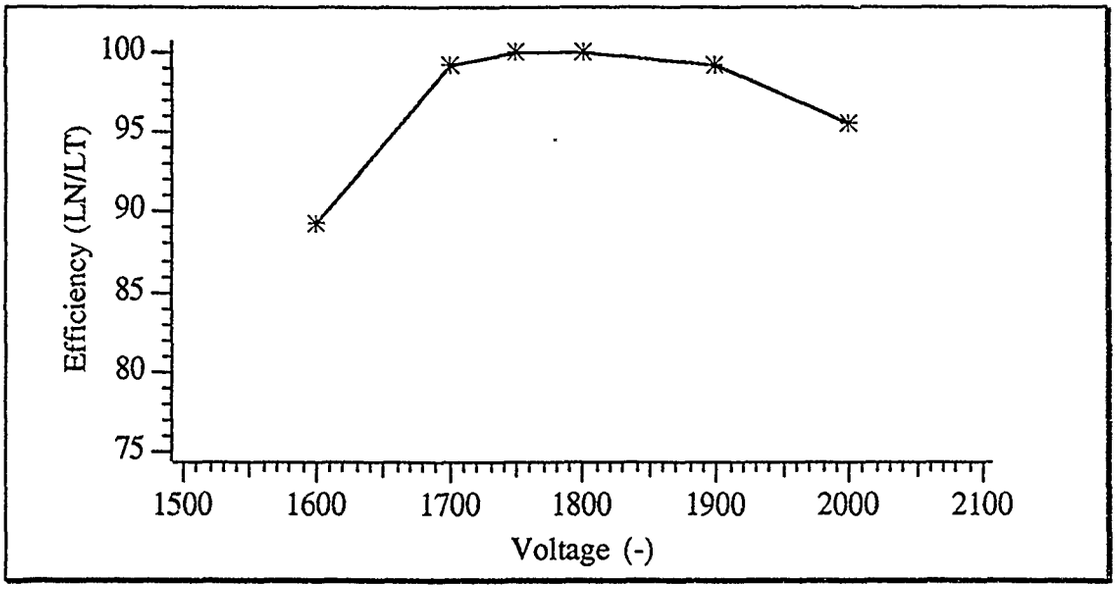

Fig. 15. Efficiency Plateau for "Thin" Mixture of Helium:Argon:Ethane.

Determination of Gas Gain

The gas gain is one of many factors that determine the total amount of charge deposited on the sense wire. Formula (5.1) allows for the determination of the total charge. The following variables are defined:

n_t is the number of primary electrons

G is the gas gain

q is the charge of the electron = 1.6×10^{-19} coulombs

α_i is the gain of the pre-amplifier chip = 175 (calculated at CEBAF)

α_f is the gain of the post amplifier = 10

ξ is the total charge deposited = (ADC peak - pedestal)•(.25pC/channel)

$$\xi = (n_p)\cdot(q)\cdot(G)\cdot(\alpha_i)\cdot(\alpha_f) \qquad (5.1)$$

The number of primaries, n_t, is determined by using the percentage of the volume of each gas and the formula for n_t (4.1). To use equation (4.1) the energy loss due to the cosmic rays (primarily muon particles at 2 GeV) must first be calculated from the Bethe-Bloch formula (5.2) or found in literature (it does not appear to be readily available). The Bethe-Bloch formula [Ref. 1] is

$$\frac{dE}{dx} = -K\frac{Z_1}{A_1}\frac{\rho}{\beta^2}\left(\ln\frac{2mc^2\beta^2E_M}{I^2(1-\beta^2)}\right) \qquad (5.2)$$

where K is a combination of fixed constants, $\frac{2\pi Nz^2e^4}{mc^2} = 0.154$ MeV $g^{-1}cm^2$, and Z_1, A_1, ρ are the atomic number, atomic mass, and density of the medium. I is the effective ionization potential (11.8 ev [Table 1] and β is the dimensionless quantity v/c in the medium (calculated for a 2 GeV muon as 0.99874).

For this system, the rest mass of the muon 105.65 Mev/c^2 is used.

The quantity E_M is a term that represents the maximum energy transfer allowed in each interaction. E_M is formally given by

$$E_M = \frac{2mc^2\beta^2}{1-\beta^2}. \qquad (5.3)$$

For a 2 GeV muon, E_M is found to be 8.374×10^4 MeV. Using the quantities for β, K, and E_M, $\frac{dE}{dx}$ is calculated to be approximately 3.704 keV/cm (a reasonable value).

Using equation (4.1), the total number of primary electrons is approximately 240 electrons for ethane. The total number of electrons for the gas mixture is determined by the following:

$$n_T = \frac{\Delta E}{W_i} = \left(\frac{\Delta E}{W_i}\right)_{He} x\ 63\% + \left(\frac{\Delta E}{W_i}\right)_{Ar} x\ 18.5\% + \left(\frac{\Delta E}{W_i}\right)_{C_2H_6} x\ 18.5\% \qquad (5.4)$$

or, after inserting values, $n_T = \frac{320}{41} \times .63 + \frac{2440}{26} \times .185 + \frac{3704}{25} \times .185 \cong 50$ ion pairs. Since the average cell length is 1.5 cm, the total number of ionized electrons per centimeter is approximately 33 electrons. Again a reasonable value is obtained. (CEBAF used the value of 100 electrons as the number of total electrons in the cell. My calculation for n_t of due to cosmic rays (muons) in 50:50 argon:ethane is 81 electrons/cm, a value within the 20-30% differences found in the literature).

ξ is determined using the spread of peak minus pedestal from the ADC plots. This value is found to be 50 channels. This value is then multiplied by the LeCroy 2249A ratio of 1 pC/ 4 channels. Therefore ξ is found to be 12.5 picocoulombs. Solving equation (5.1) for G gives:

$$\text{Gas gain} = \frac{12.5 \times 10^{-12} pC}{(.05)\cdot(10)\cdot(175)\cdot(1.6 \times 10^{-19} coul)\cdot(33\ e^-)} = 2.71 \times 10^4 \qquad (5.5)$$

Conducting the Measurement

The process of the measurement required several simple yet careful steps. Initial data were recorded in the logbook. Figure 16 depicts a typical log sheet and the required data entries for each run.

RunXX.dat			
Time			
Gas Type			
Cylinder Pressure			
Flowrate			
Chamber Gas Press [in. H2O]			
Preamp Voltage [V]			
Current [mA]			
Field Wire Voltage [V]			
Field Wire Current [mA]			
Guard Wire Voltage [V]			
Guard Wire Current [mA]			
Discriminator Module 1 [mV]			
Discriminator Module 2 [mV]			
Scintillator Voltage Top [V]			
Scintillator Voltage Bottom [V]			
Scintillator Discriminator Top [mV]			
Scintillator Discriminator Bottom [mV]			
Magnet Voltage [V]			
Magnet Current [A]			
Polarity (A or B)			
Chamber Angle			
Hall Probe [V]			

Figure 16. Pre-run Data Entry Sheet.

As the data were being recorded, the start of the run was initialized via the computer. The following items were entered at the start of the program TRACK: the run number, field wire voltage , discriminator voltage, distance of error for tracks close to a border, time offset T0, maximum flight time of the particle, the desired excluded layer, the non-instrumented wires, and any pertinent comments. The experimental run was initialized by running the TRACK program.

Care had to be exercised when entering the data into the computer. Errors such as typing integers for real numbers caused the program to crash. To check if the program was entered correctly, a statistics sheet was called to the screen. An additional inspection was to observe the CAMAC crate's LEDs. If they "blinked" as an event was taking place, the hardware was properly receiving signal. During a run,

the TRACK program allowed viewing of a raw track event, the current statistics, residuals of the six layers or excluded layer, ADC and TDC histograms, and the time-distance plots for the six layers or excluded layer.

Due to the time allotted for the entire experiment, each run duration had to be planned so that a maximum number of runs could be made. This included the run time for plateau runs and time needed for purging of the chamber when a new gas mixture was introduced. Therefore each run was allowed to continue for a fixed time duration.

At the end of a run, the TRACK program was stopped (not exited!). At this point, collected data for the run was printed for analysis purposes. The standard outputs were the XTPLOT, XTPLOT/E, RESP, RESP/E, and the statistics sheet. Exiting the TRACK program was executed by typing exit. This "reset" the computer for the next run. Between runs, backup copies of the data files were made and sent to the experiment file on BNLDAG.

The entire Brookhaven experiment lasted over two weeks. The first part of the experiment was to determine the working characteristics of the one meter drift chamber using argon:ethane in a high magnetic field at various angles, θ = 0, 10, 20, and 30 degrees. The second part of the experiment dealt with studying a helium dominated gas mixture in the magnetic field. Two days of magnet time was allotted for this part. Since part two of this experiment is the basis of this thesis, the experiment is described with the run schedule and accompanying remarks for the helium:argon:ethane runs.

RUN SCHEDULE

Night #1 — Purged chamber with helium. To prevent sparking inside the chamber, the field and guard voltages were set to zero.

Day #1 — Calibrate flowmeters for new mixture while flowing the new mixture into the chamber. The flow rates were fixed as the the following: (50:50) argon: ethane 52 cc/min, helium 89 cc/min. Established a working plateau plateau good enough for use with the magnet. Conducted runs at B = 0 and B = 1.5 Tesla.

Night #2 — Cut the flow rate of the argon:ethane by 50 percent. Flow rates were set as follows: argon:ethane 27 cc/min, helium 114 cc/min.

Day #2 — After purging with the new gas mixture, plateau runs were conducted through the morning. It was observed that this new mixture provided more events that had to be "thrown out" because of adjacent cells signalling. This was probably due to a mixture that was too rich in helium: argon and not enough quencher to absorb the extra ionizations taking place inside the chamber. Runs were conducted at B = 0 and B = 1.5 T.

End of the experiment.

CHAPTER VI

ANALYSIS OF DATA

General

Data is analyzed in reference to a single event; that event being a cosmic ray passing through the scintillators and the drift chamber. The duration of the event was determined by the start signal of the top scintillator and the stop signal of the bottom scintillator. This time difference between the two scintillators was the measure of time needed to make a calculation of the distance from a particular sense wire where ionization took place. The calculations were based on an initial velocity function which was obtained from literature of drift velocities of electrons in gas mixtures. This velocity function was essentially the "template" which provided a guess as to where the ionization originated in reference to a sense wire.

Using this initial velocity function and the timing data, a least squares fit to a straight track was obtained for each sense wire that provided a signal. Using figure 8, the distance from a signalling sense wire where the ionization took place is calculated from the time difference of the event. This distance is depicted by the concentric circle surrounding the sense wire. Recognizing the left-right pattern of the sense wire, a best fit line tangent to each circle is drawn. This line, a least squares fit, is a calculated track.

From the information of the track, an XTPLOT for the run was created. This plot showed the calculated distance of closest approach (path between the wires as depicted by the tangent circles and the straight line fit) versus the time difference for each wire detecting the electron swarm created near it.

To analyze the data from this experiment, the velocity function had to be modified so that a minimum residual of all the layers as well as the excluded layer would be obtained. The residual is a measure of the width of the drift velocity and is defined as

$$\sum \frac{(\text{measured value - the average value})^2}{\text{total number of points}} . \qquad (6.1)$$

To do this process, the program TRACK_OFFLINE [Ref. 18] program was used. This analysis process was an iterative one. Using an initial graph output, XTPLOT, nine evenly distributed (x,t) points were chosen which best described the velocity of the electrons. These points were chosen such that they denoted the mean of the velocity function at a particular x value and a time value. The nine (x,t) points were edited into the velocity function, Velocity_HeBxx.dat (xx being either 0 or 15 depending on the magnetic field setting for the run).

The program was run as required with each new velocity function. If the (x,t) points were chosen carefully, the dashed line that delineates the velocity function should match the thousands of data (x,t) points on the XTPLOT. As a result of the establishment of the velocity function, the residual values on the statistics sheet will decrease to a minimum.

This method of analysis is self-consistent based on the premise that tracks which pass a sense wire exactly provide data points which do not require calculation. Sense wires which signal away from a direct "hit" determine the distance of closest approach by incorporating the position of the direct "hit". Therefore, regardless of the velocity function, the direct "hit" must continue to register as such. Using this iterative process allows for improving the actual linear approximation of the track and its improvements are observed in the residual value.

Once the velocity function was established, the next factor to have an impact on the residuals was the time offset value, a reference which sets a zero start time for each run. The inherent nature of the electronics within the system requires a certain amount of time for the signal to be amplified, delayed for separation and registered by the acquistion system. This time is acccunted for by setting an average time offset. By replaying each run, the T zero (T0) was increased or decreased as an input value for software calculation. Again, once the correct T0 was obtained, the residual values showed a minimum value.

The Statistics, XTPLOT, XTPLOT/E, RESP, RESP/E sheets are shown for helium:argon:ethane mixtures at B = 0 and B = 1.5 T. For comparison purposes, the corresponding plots are provided for (50:50) argon:ethane.

```
                    TRACK  SYSTEM  STATUS          RUN#      100
                    ----------------------
                      10:44:47 28-NOV-90

PARAMETERS:
                  GUARD                SENSE                  FIELD
  Voltage(v):                                                 1900.0
  Discriminator(mv):                                            20.00
  Cell Border(cm):                                               0.06
  Mean TDC Cut[t0](ns):                                         13.00
  Time Scale(ns):                                               600.0
  Excluded Layer:                                                   3
  Excluded wires:                                  33 34 35 36  0
  Relative TDC Offsets[t00](ns):
   Channel    1 - 6:    0.00    0.00    0.00    0.00    0.00    0.00
   Channel    7 - 12:   0.00    0.00    0.75    0.75    0.75    0.75
   Channel   13 - 18:   0.75    0.75    0.75    0.75   -0.25   -0.25
   Channel   19 - 24:  -0.25   -0.25   -0.25   -0.25   -0.25   -0.25
   Channel   25 - 30:   3.50    3.50    3.50    3.50    3.50    3.50
   Channel   31 - 36:   3.50    3.50    0.00    0.00    0.00    0.00
      v0 :          1900.00
   thmin :           0.0000          thmax :                  0.5236
   timev :     0.000   140.000   200.000   215.000   320.000
             360.000   400.000   480.000   520.000
      xv :   -0.040 0.379 0.518 0.549 0.711 0.768 0.811 0.876 0.891
             -0.040 0.379 0.518 0.549 0.711 0.800 0.850 0.922 0.930

ANALYSIS RESULTS:
  Number of Triggers:                                             782
  Total tracks through layer:(T)                                  334
  Tracks through cells which did not signal:(N)                    27
  Percentage: (N/T)                                              8.08%
  Cells signalling which did not contain tracks:(M)                 1
  Percentage: (M/T)                                              0.32%
  Number of inefficiencies with maxtim < t      < timeout:          0
  Number of inefficiencies with track near border (<.060 cm):      18

  Number of tracks through layer:(LT)                             225
  Number of times layer fired:(LN)                                223
  Percentage: (LN/LT)                                           99.11%
  Total cells signalling:                                         308
  Number of inefficiencies with track near cell (<.060 cm):         0

  The average residual (cm):                          -0.1721E-02
  10-bin rms value (cm):                               0.2135E-01
  The average residual of excluded layer(cm):          0.9758E-02
  10-bin rms value of excluded layer(cm):              0.2340E-01

COMMENTS:
  (63:18.5:18.5) Helium:Argon:Ethane at B=0.
```

Fig. 17. Statistics for Helium:Argon:Ethane Run at B = 0.

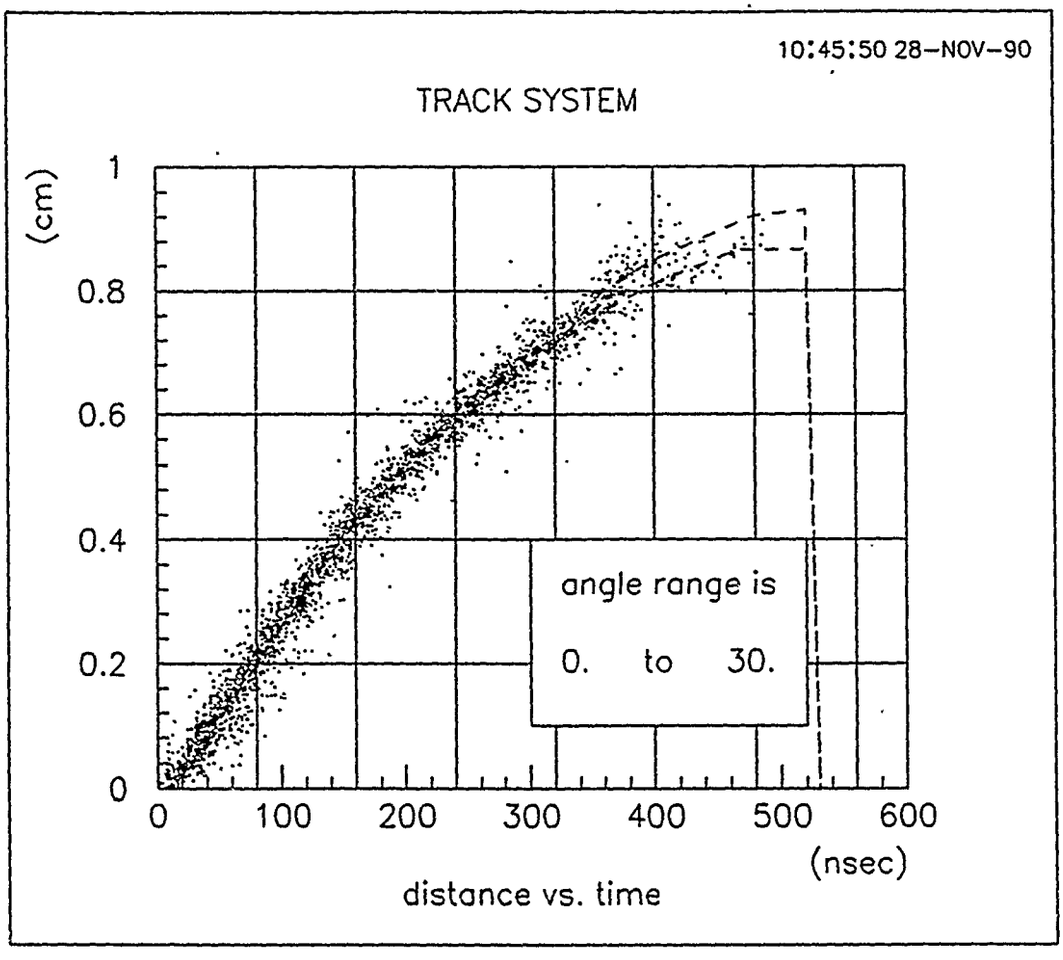

Fig. 18. XTPLOT for Helium:Argon:Ethane Run at B = 0.

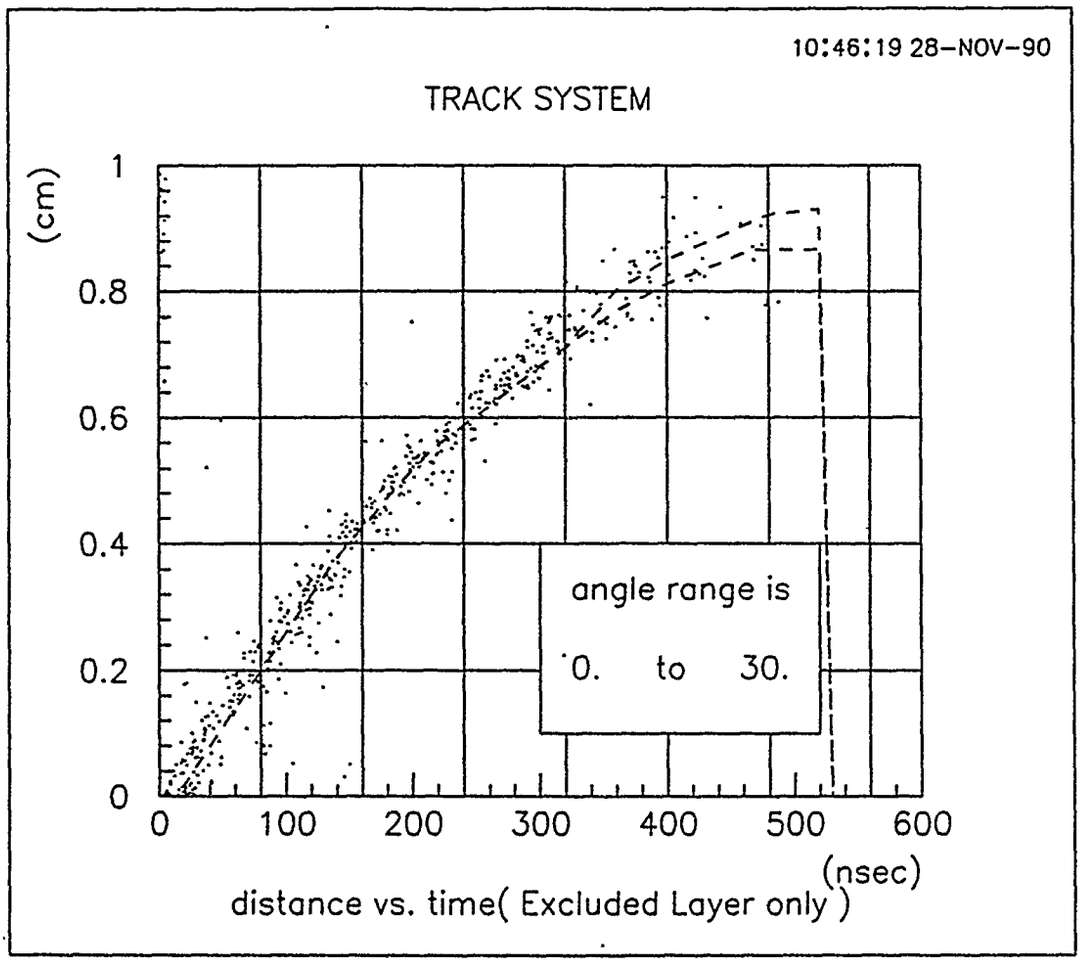

Fig. 19. XTPLOT of the Excluded Layer for Helium:Argon:Ethane Run at B = 0.

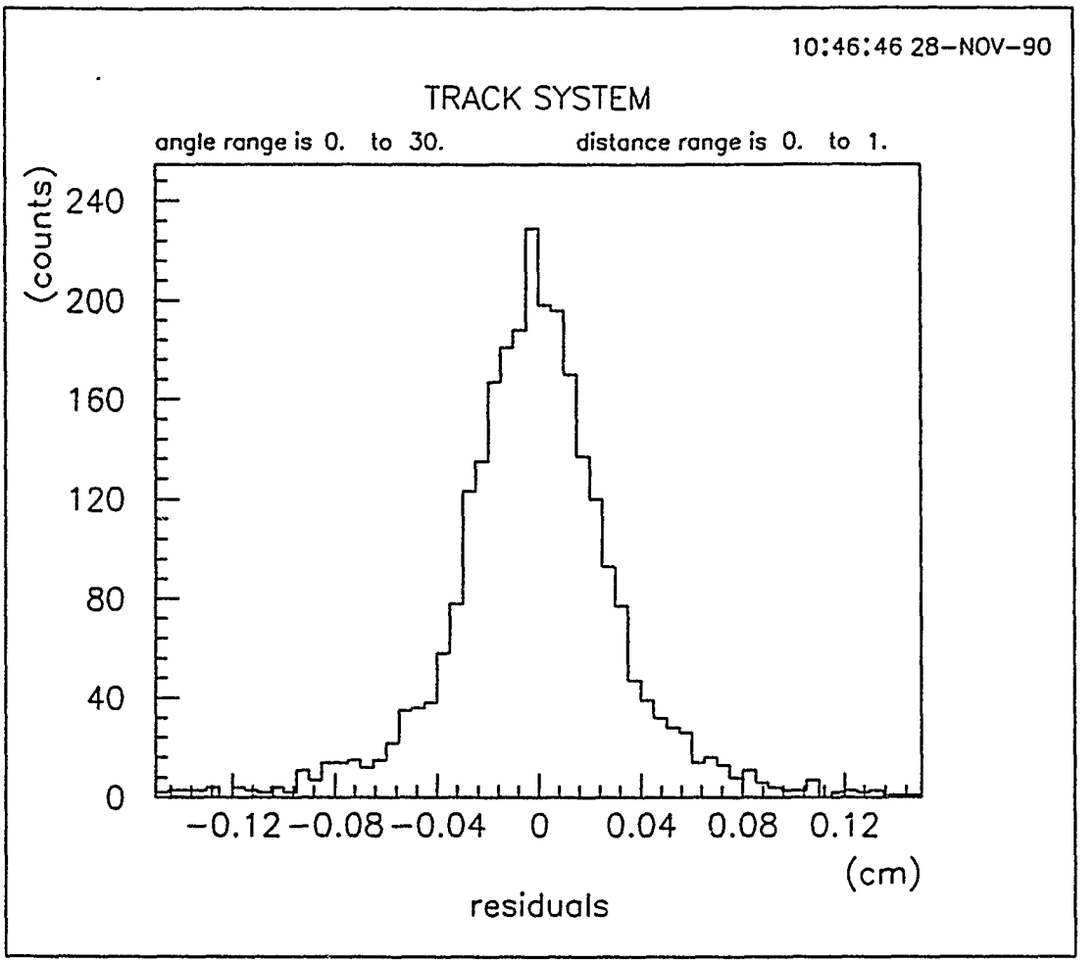

Fig. 20. Residual Histogram for Helium:Argon:Ethane Run at B = 0.

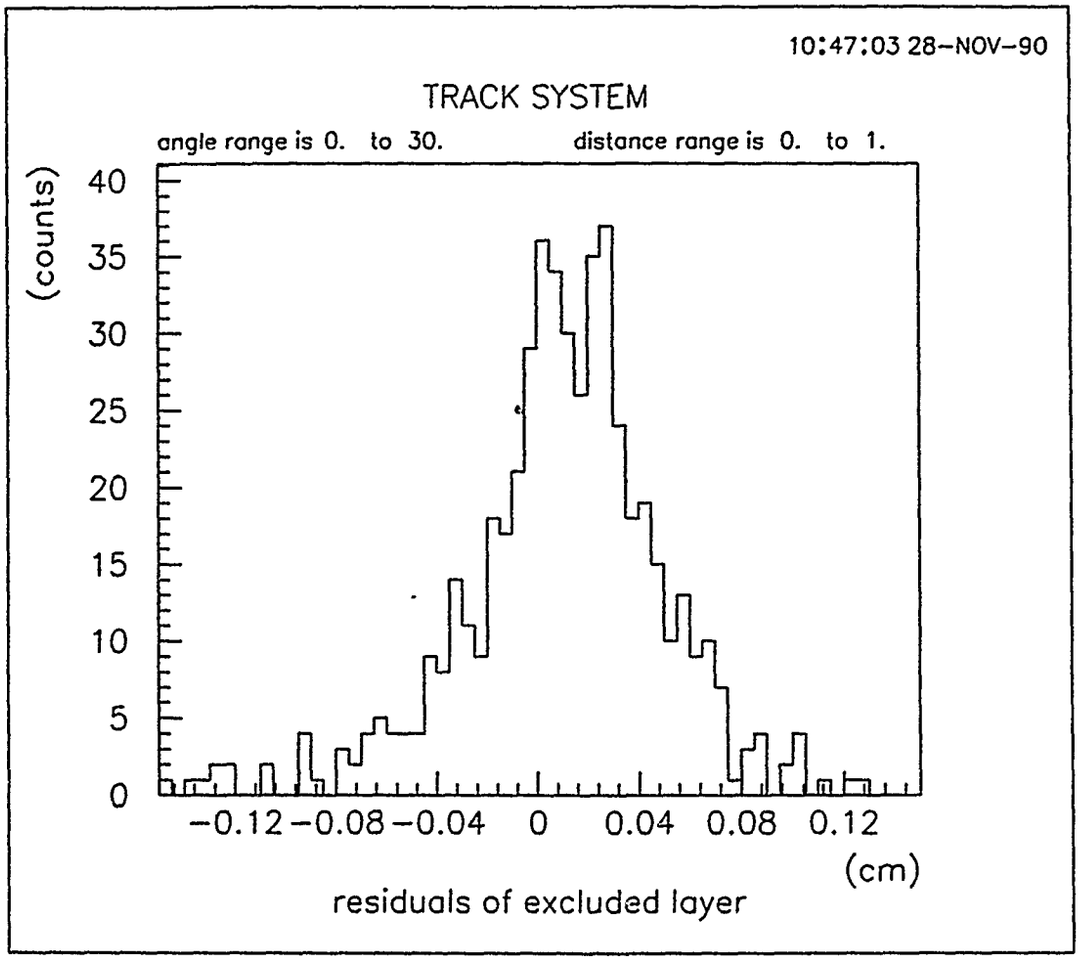

Fig. 21. Excluded Layer Residual Histogram for Helium:Argon:Ethane Run at B = 0.

```
                    TRACK  SYSTEM  STATUS          RUN#      102
                   ----------------------
                     10:56:54 28-NOV-90

PARAMETERS:
                        GUARD                SENSE                  FIELD
  Voltage(v):                                                      2000.0
  Discriminator(mv):                                                20.00
  Cell Border(cm):                                                   0.06
  Mean TDC Cut[t0](ns):                                             13.00
  Time Scale(ns):                                                   600.0
  Excluded Layer:                                                       3
  Excluded wires:                                  33 34 35 36  0
  Relative TDC Offsets[t00](ns):
   Channel    1 - 6:    0.00    0.00    0.00    0.00    0.00    0.00
   Channel    7 - 12:   0.00    0.00    0.75    0.75    0.75    0.75
   Channel   13 - 18:   0.75    0.75    0.75    0.75   -0.25   -0.25
   Channel   19 - 24:  -0.25   -0.25   -0.25   -0.25   -0.25   -0.25
   Channel   25 - 30:   3.50    3.50    3.50    3.50    3.50    3.50
   Channel   31 - 36:   3.50    3.50    0.00    0.00    0.00    0.00
      v0 :          2000.00
   thmin :           0.0000          thmax :                  0.5236
   timev :     0.000    52.000   110.000   180.000   240.000
             320.000   400.000   480.000   520.000
      xv :   -0.040 0.164 0.299 0.434 0.522 0.643 0.764 0.884 0.922
             -0.040 0.164 0.299 0.438 0.537 0.665 0.791 0.918 0.983

ANALYSIS RESULTS:
  Number of Triggers:                                               2389
  Total tracks through layer:(T)                                    1246
  Tracks through cells which did not signal:(N)                       66
  Percentage: (N/T)                                                5.30%
  Cells signalling which did not contain tracks:(M)                    4
  Percentage: (M/T)                                                0.34%
  Number of inefficiencies with maxtim < t      < timeout:             0
  Number of inefficiencies with track near border (<.060 cm):         39

  Number of tracks through layer:(LT)                               825
  Number of times layer fired:(LN)                                  822
  Percentage: (LN/LT)                                             99.64%
  Total cells signalling:                                          1184
  Number of inefficiencies with track near cell (<.060 cm):           3

  The average residual (cm):                              -0.1733E-02
  10-bin rms value (cm):                                   0.2057E-01
  The average residual of excluded layer(cm):              0.1831E-02
  10-bin rms value of excluded layer(cm):                  0.2336E-01

COMMENTS:
  (63:18.5:18.5) Helium:Argon:Ethane at B=1.5.
```

Fig. 22. Statistics for Helium:Argon:Ethane Run at B = 1.5.

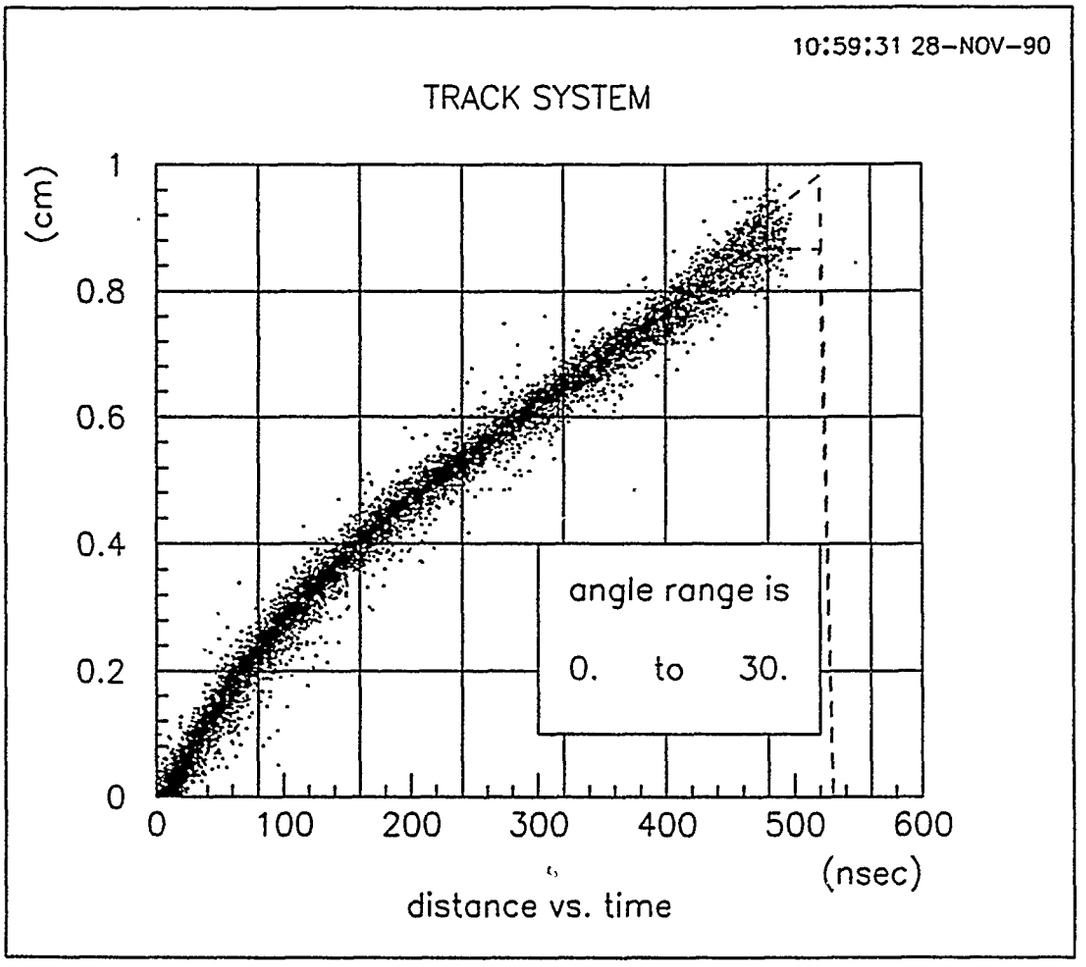

Fig. 23. XTPLOT for Helium:Argon:Ethane Run at B = 1.5.

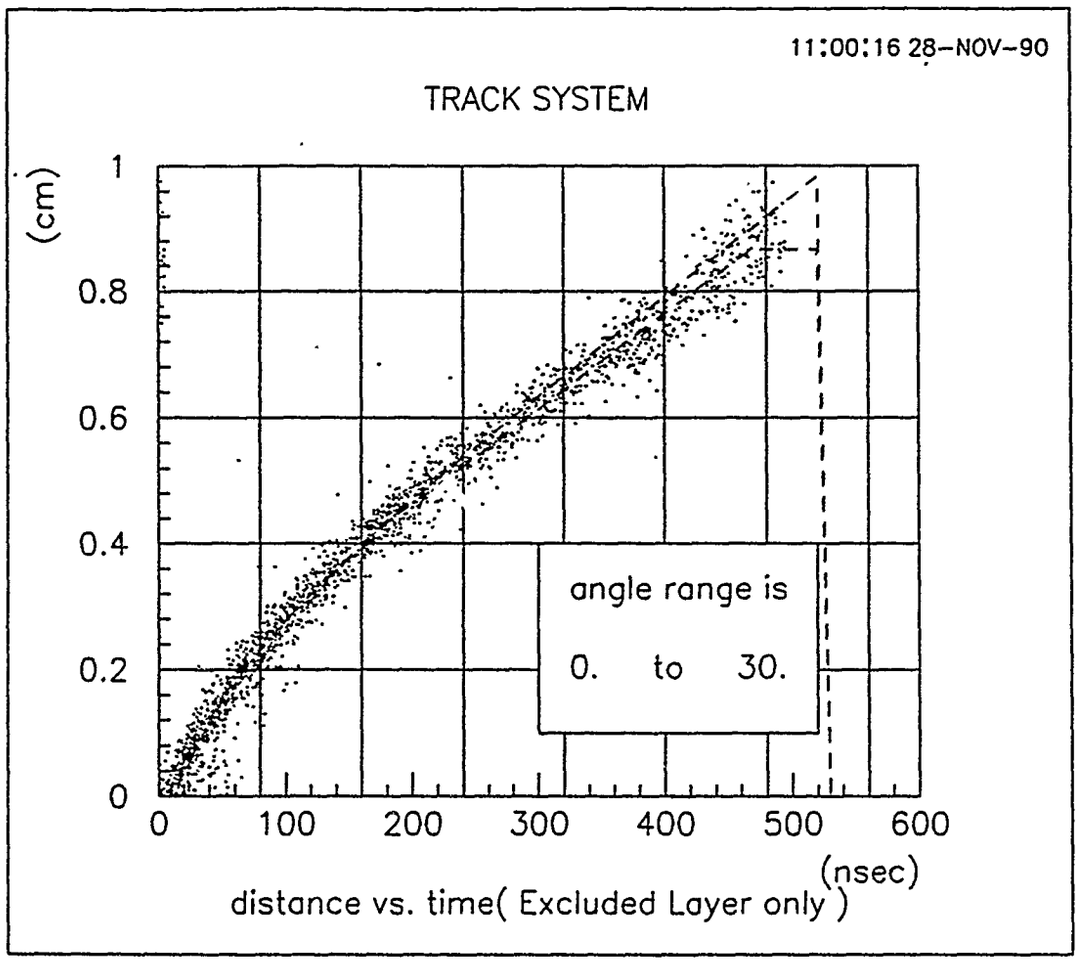

Fig. 24. XTPLOT of the Excluded Layer for Helium:Argon:Ethane Run at B = 1.5.

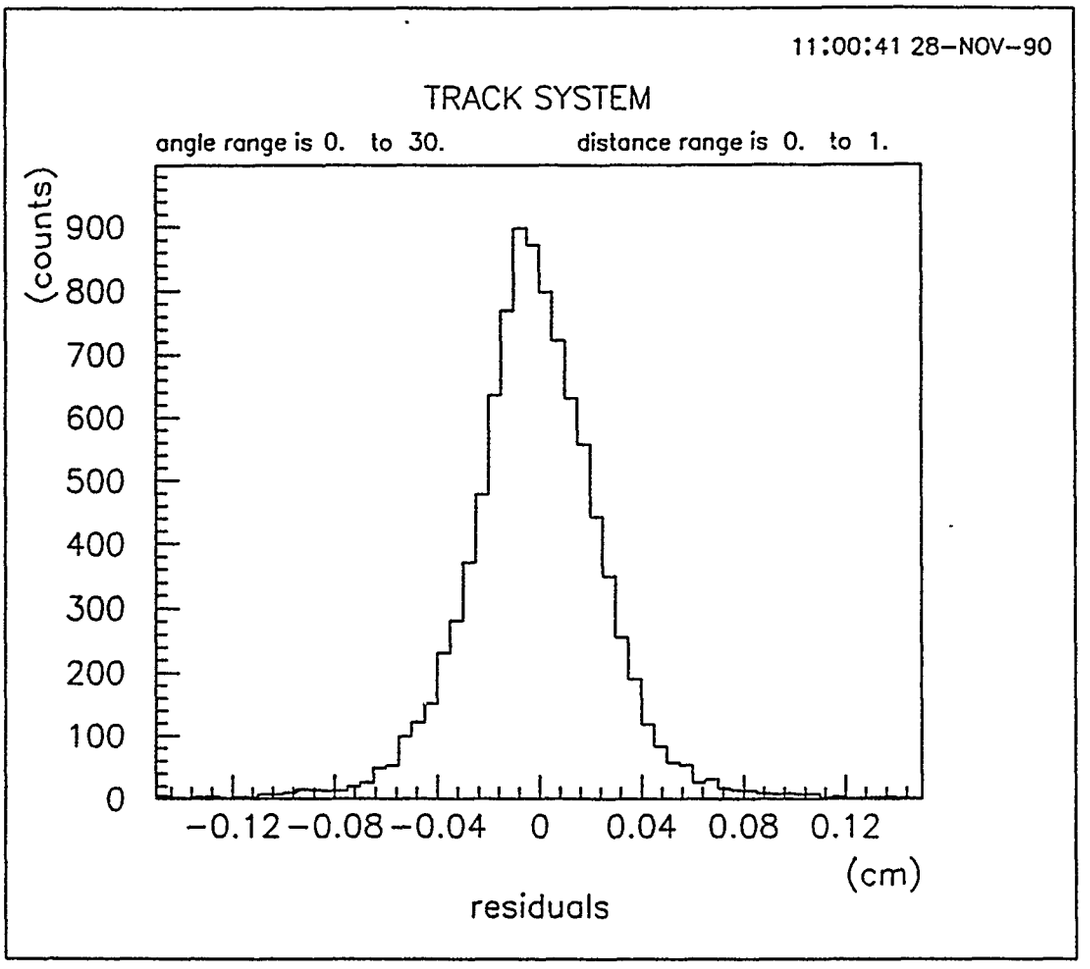

Fig. 25. Residual Histogram for Helium:Argon:Ethane Run at B = 1.5.

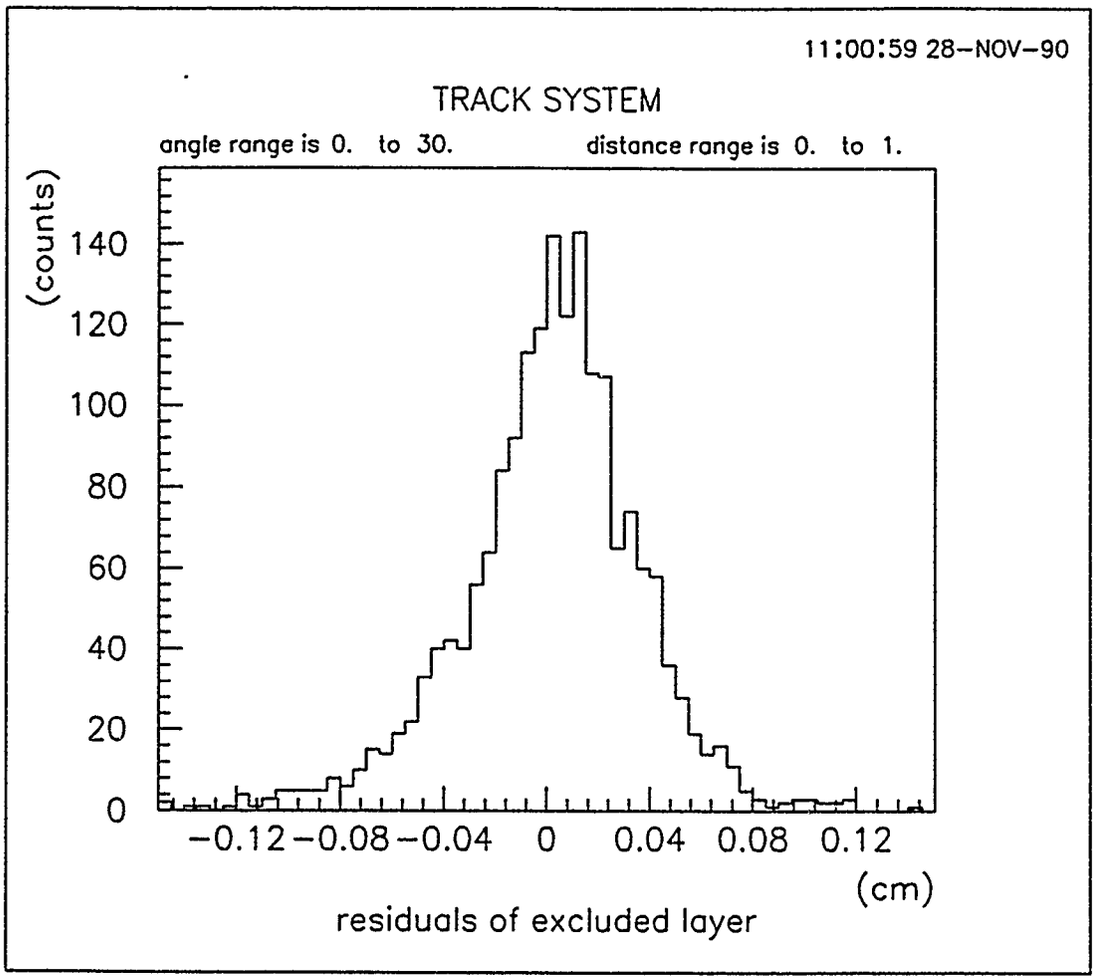

Fig. 26. Excluded Layer Residual Histogram for Helium:Argon:Ethane Run at B = 1.5.

```
                    TRACK  SYSTEM  STATUS          RUN#       37
                    ----------------------
                      11:36:33 28-NOV-90

PARAMETERS:
                    GUARD                SENSE                    FIELD
  Voltage(v):                                                     2550.0
  Discriminator(mv):                                                20.00
  Cell Border(cm):                                                   0.06
  Mean TDC Cut[t0](ns):                                             13.00
  Time Scale(ns):                                                   600.0
  Excluded Layer:                                                       3
  Excluded wires:                                  33 34 35 36  0
  Relative TDC Offsets[t00](ns):
   Channel    1 - 6:    0.00    0.00    0.00    0.00    0.00    0.00
   Channel    7 - 12:   0.00    0.00    0.75    0.75    0.75    0.75
   Channel   13 - 18:   0.75    0.75    0.75    0.75   -0.25   -0.25
   Channel   19 - 24:  -0.25   -0.25   -0.25   -0.25   -0.25   -0.25
   Channel   25 - 30:   3.50    3.50    3.50    3.50    3.50    3.50
   Channel   31 - 36:   3.50    3.50    0.00    0.00    0.00    0.00
      v0 :          2550.00
   thmin :           0.0000          thmax :                   0.5240
   timev :     0.000    40.000    80.000   120.000   160.000
             200.000   240.000   280.000   300.000
      xv :   -0.040 0.192 0.380 0.560 0.670 0.780 0.840 0.865 0.866
             -0.040 0.192 0.380 0.560 0.690 0.830 0.915 0.999 1.000

ANALYSIS RESULTS:
  Number of Triggers:                                              7771
  Total tracks through layer:(T)                                   3276
  Tracks through cells which did not signal:(N)                      94
  Percentage: (N/T)                                               2.87%
  Cells signalling which did not contain tracks:(M)                  34
  Percentage: (M/T)                                               1.06%
  Number of inefficiencies with maxtim < t      < timeout:            0
  Number of inefficiencies with track near border (<.060 cm):        85

  Number of tracks through layer:(LT)                              2170
  Number of times layer fired:(LN)                                 2170
  Percentage: (LN/LT)                                            100.00%
  Total cells signalling:                                          3216
  Number of inefficiencies with track near cell (<.060 cm):           9

  The average residual (cm):                              -0.4656E-02
  10-bin rms value (cm):                                   0.2393E-01
  The average residual of excluded layer(cm):              0.2144E-01
  10-bin rms value of excluded layer(cm):                  0.2631E-01

COMMENTS:
  (50:50) Argon:Ethane at B=0.
```

Fig. 27. Statistics for Argon:Ethane Run at B = 0.

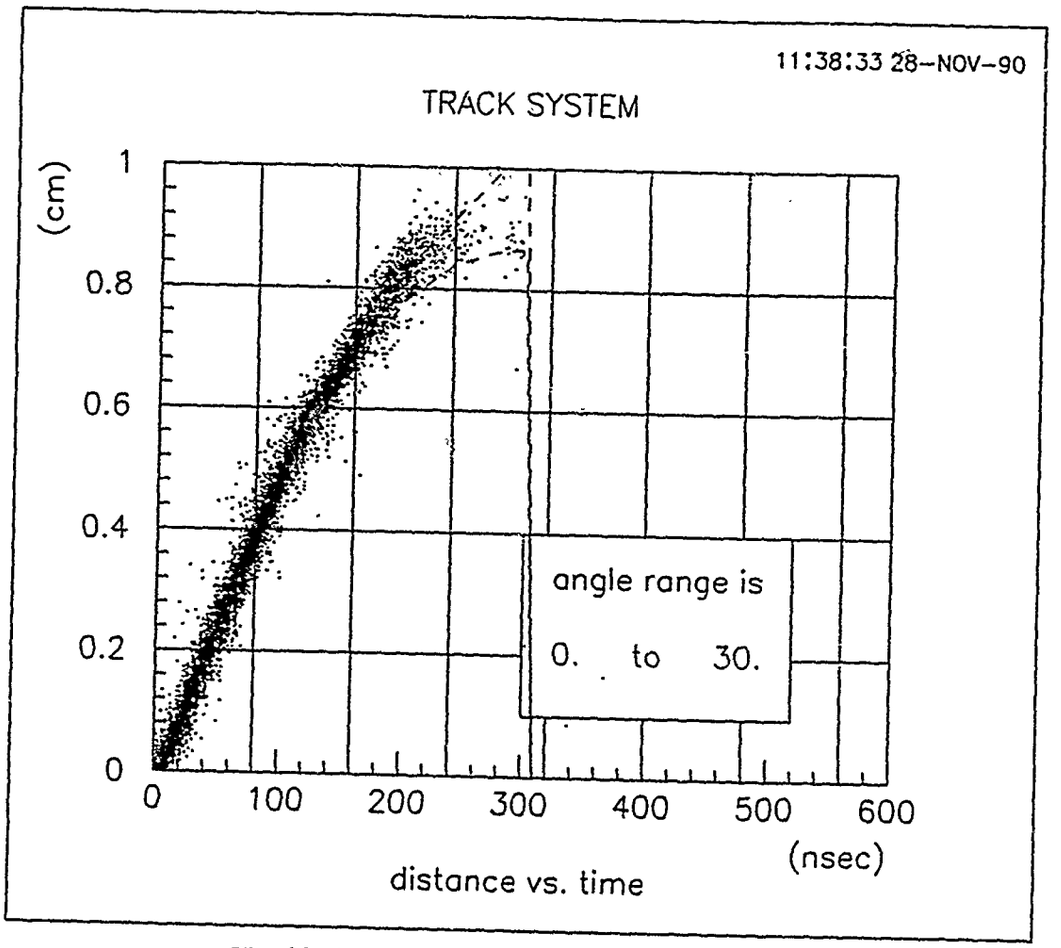

Fig. 28. XTPLOT for Argon:Ethane Run at B = 0.

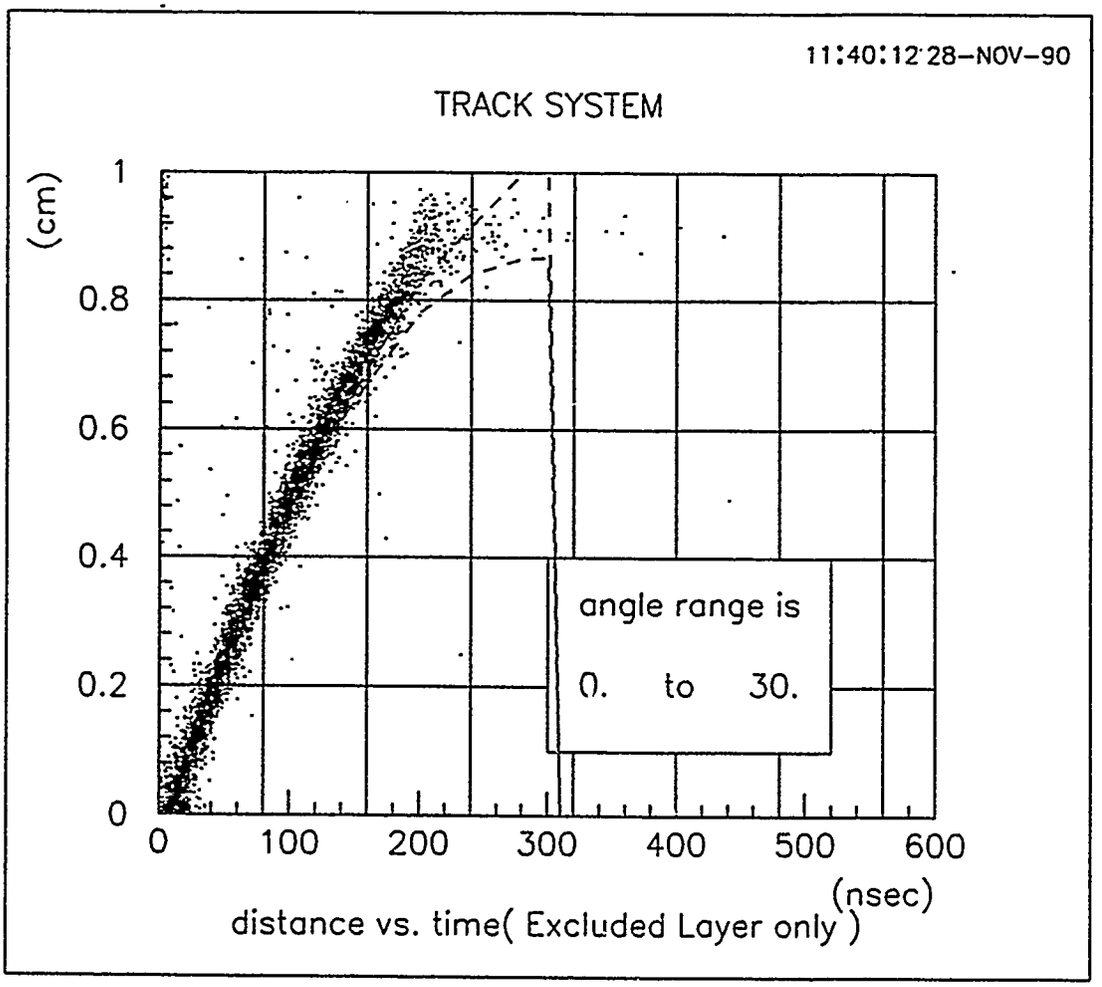

Fig. 29. XTPLOT of the Excluded Layer for Argon:Ethane Run at B = 0.

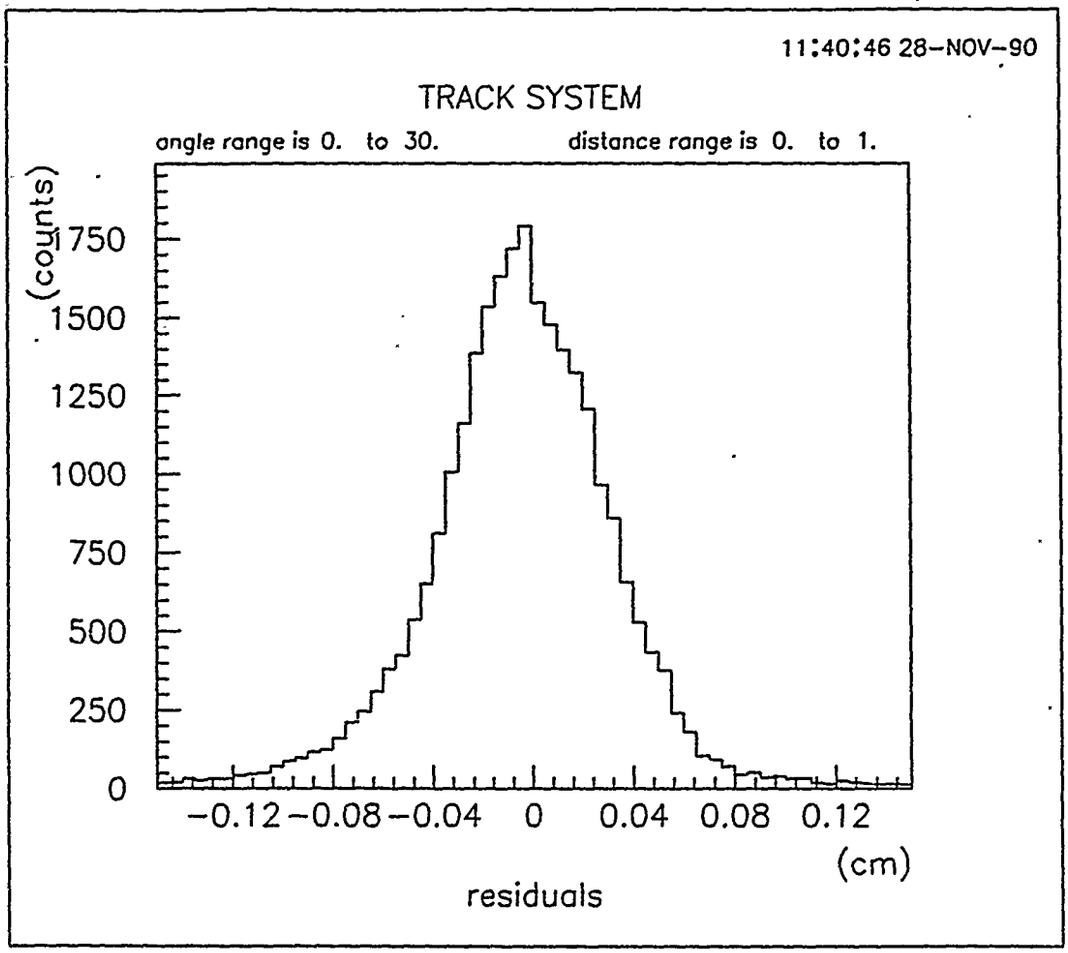

Fig. 30. Residual Histogram for Argon:Ethane Run at B = 0.

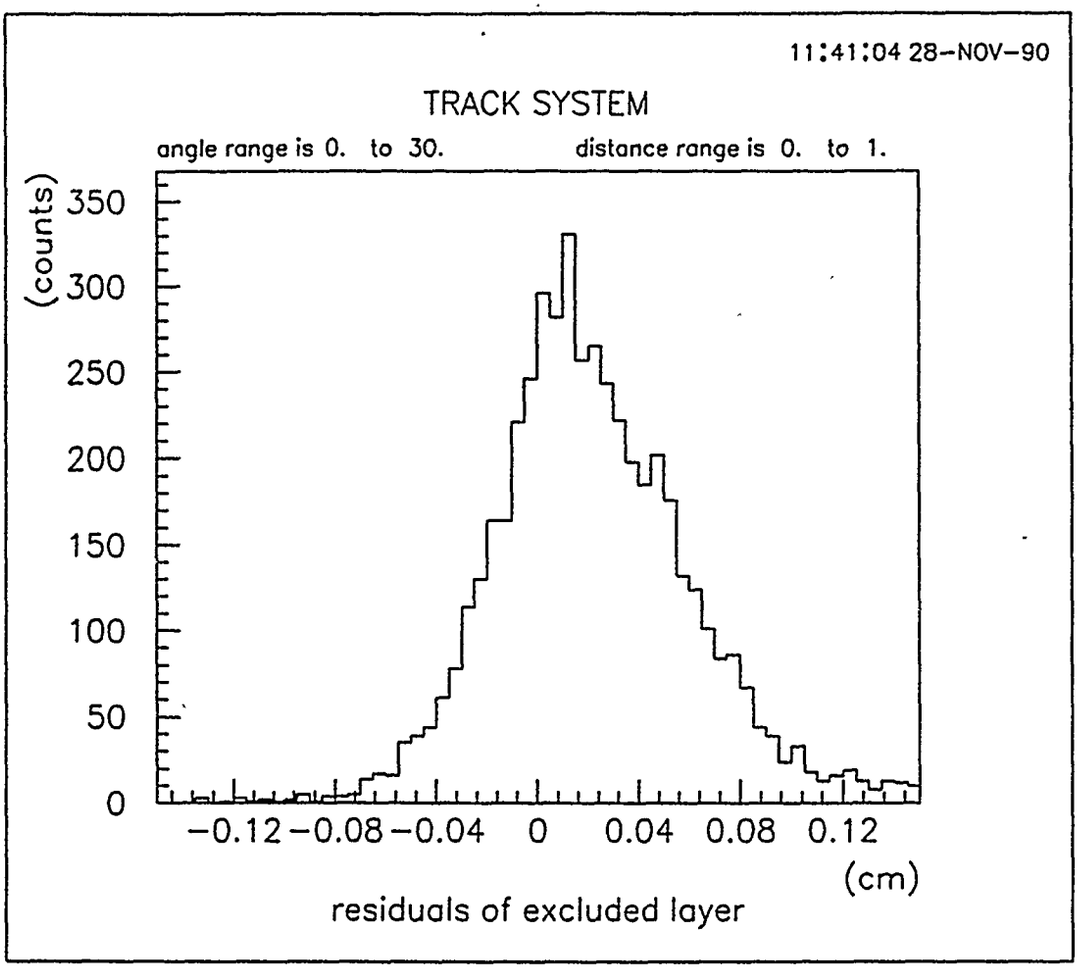

Fig. 31. Excluded Layer Residual Histogram for Argon:Ethane Run at B = 0.

```
                    TRACK  SYSTEM  STATUS          RUN#      38
                    ----------------------
                      11:10:03 28-NOV-90

PARAMETERS:
                  GUARD                SENSE                  FIELD
  Voltage(v):                                                2550.0
  Discriminator(mv):                                           20.00
  Cell Border(cm):                                              0.06
  Mean TDC Cut[t0](ns):                                        13.00
  Time Scale(ns):                                             600.0
  Excluded Layer:                                                 3
  Excluded wires:                                  33 34 35 36  0
  Relative TDC Offsets[t00](ns):
   Channel    1 - 6:    0.00    0.00    0.00    0.00    0.00    0.00
   Channel    7 - 12:   0.00    0.00    0.75    0.75    0.75    0.75
   Channel   13 - 18:   0.75    0.75    0.75    0.75   -0.25   -0.25
   Channel   19 - 24:  -0.25   -0.25   -0.25   -0.25   -0.25   -0.25
   Channel   25 - 30:   3.50    3.50    3.50    3.50    3.50    3.50
   Channel   31 - 36:   3.50    3.50    0.00    0.00    0.00    0.00
      v0 :          2550.00
   thmin :           0.0000          thmax :                  0.5236
   timev :     0.000    54.000    97.600   208.500   265.300
             340.200   367.600   409.300   452.000
      xv :  -0.040 0.235 0.382 0.600 0.680 0.788 0.863 0.929 1.000
            -0.040 0.235 0.382 0.600 0.724 0.831 0.920 1.000 1.090

ANALYSIS RESULTS:
  Number of Triggers:                                          1837
  Total tracks through layer:(T)                                866
  Tracks through cells which did not signal:(N)                   6
  Percentage: (N/T)                                            0.69%
  Cells signalling which did not contain tracks:(M)              63
  Percentage: (M/T)                                            6.83%
  Number of inefficiencies with maxtim < t      < timeout:        0
  Number of inefficiencies with track near border (<.060 cm):     2

  Number of tracks through layer:(LT)                          559
  Number of times layer fired:(LN)                             559
  Percentage: (LN/LT)                                       100.00%
  Total cells signalling:                                      923
  Number of inefficiencies with track near cell (<.060 cm):     34

  The average residual (cm):                          -0.5898E-02
  10-bin rms value (cm):                               0.2075E-01
  The average residual of excluded layer(cm):          0.6374E-02
  10-bin rms value of excluded layer(cm):              0.2490E-01

COMMENTS:
  (50:50) Argon:Ethane at B=1.5.
```

Fig. 32. Statistics for Argon:Ethane Run at B = 1.5.

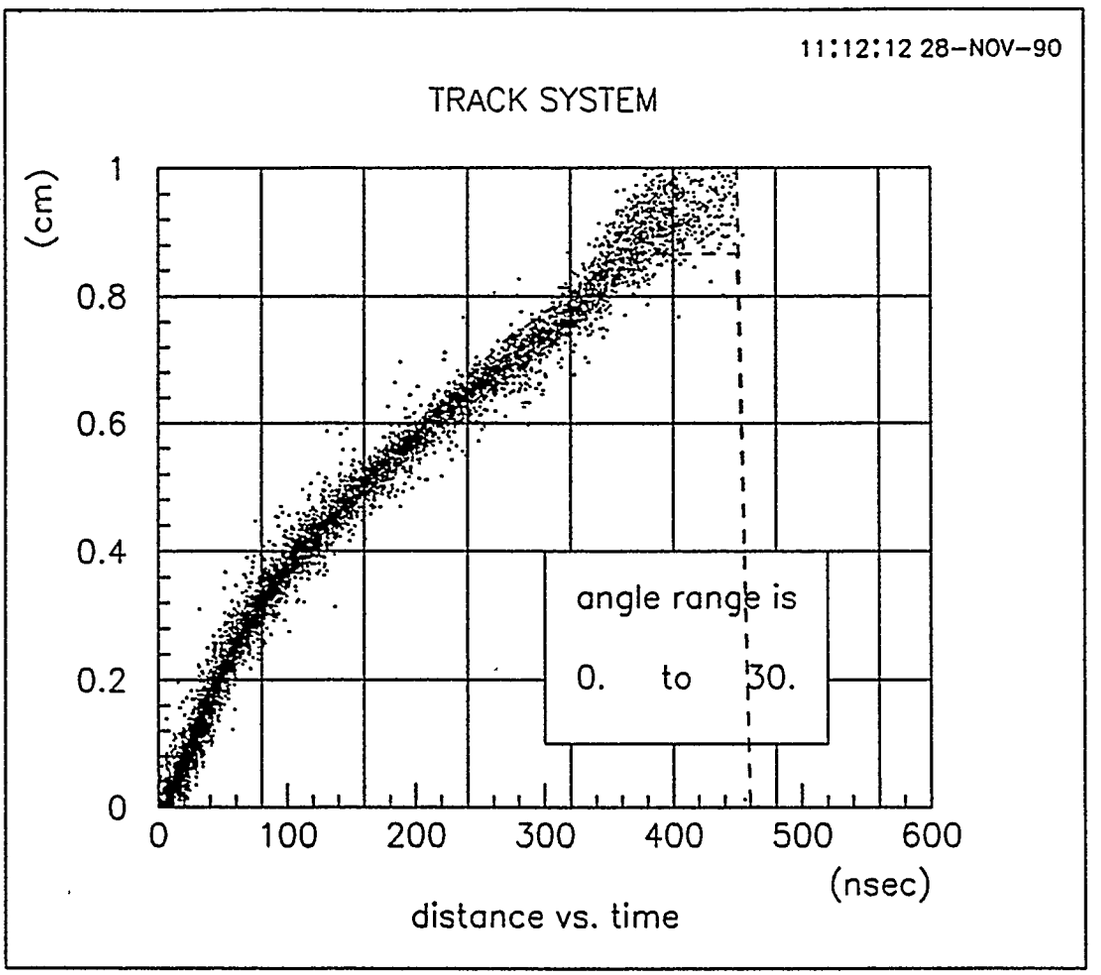

Fig. 33. XTPLOT for Argon:Ethane Run at B = 1.5.

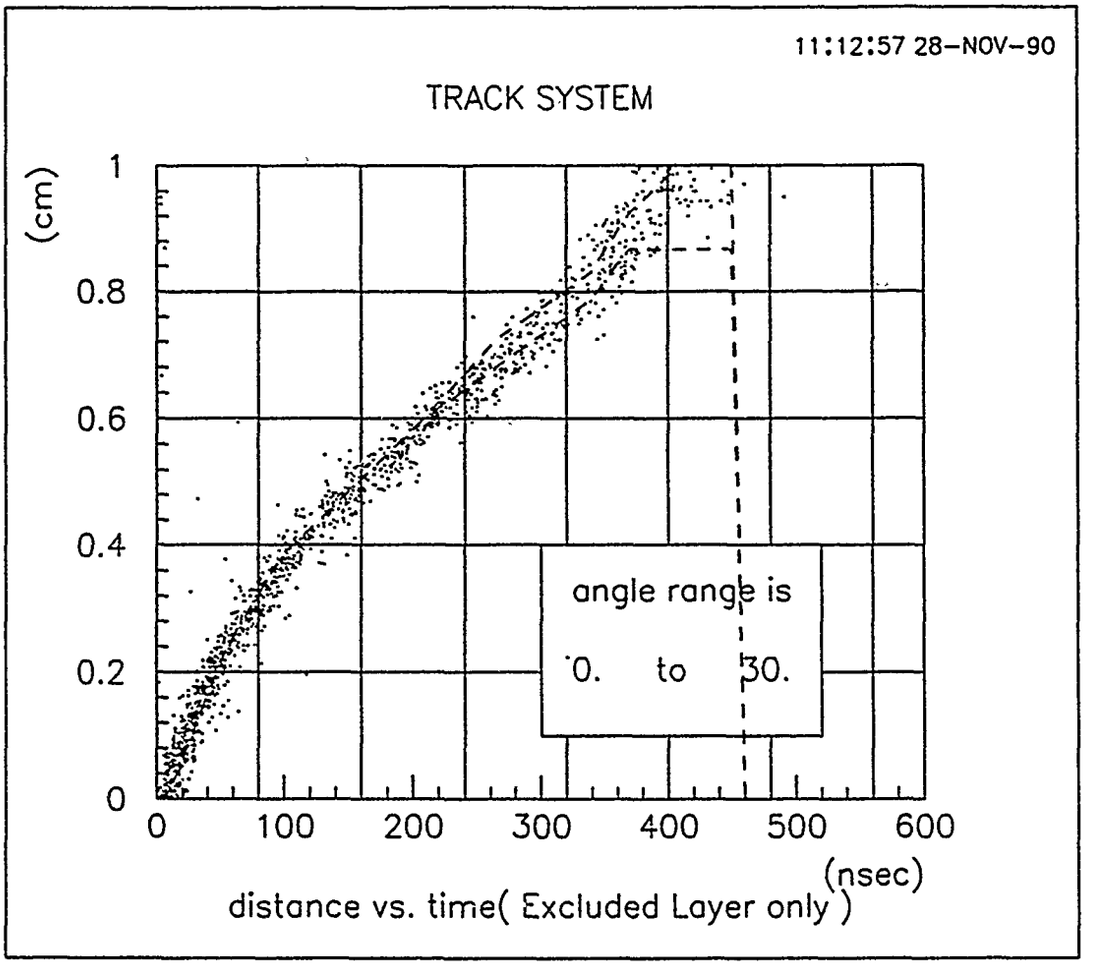

Fig. 34. XTPLOT of the Excluded Layer for Argon:Ethane Run at B = 1.5.

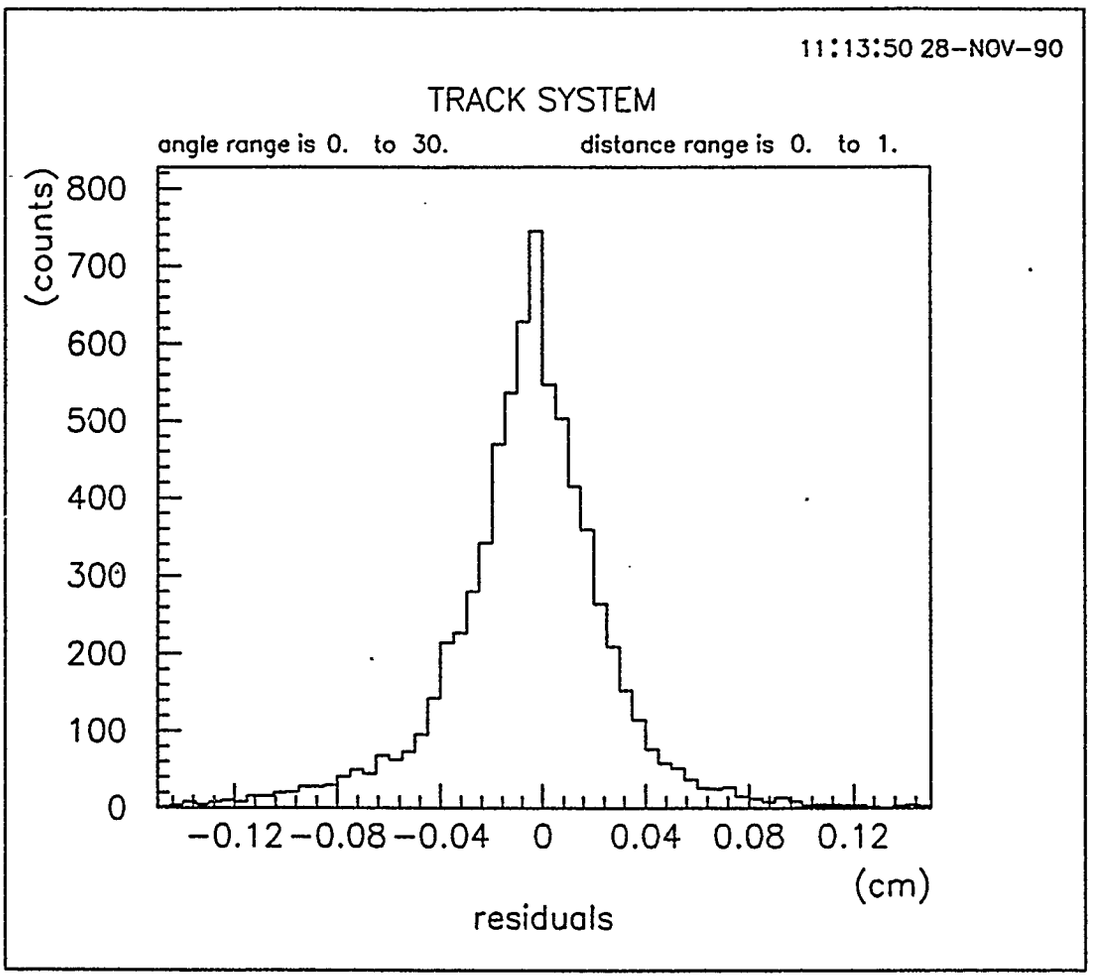

Fig. 35. Residual Histogram for Argon:Ethane Run at B = 1.5.

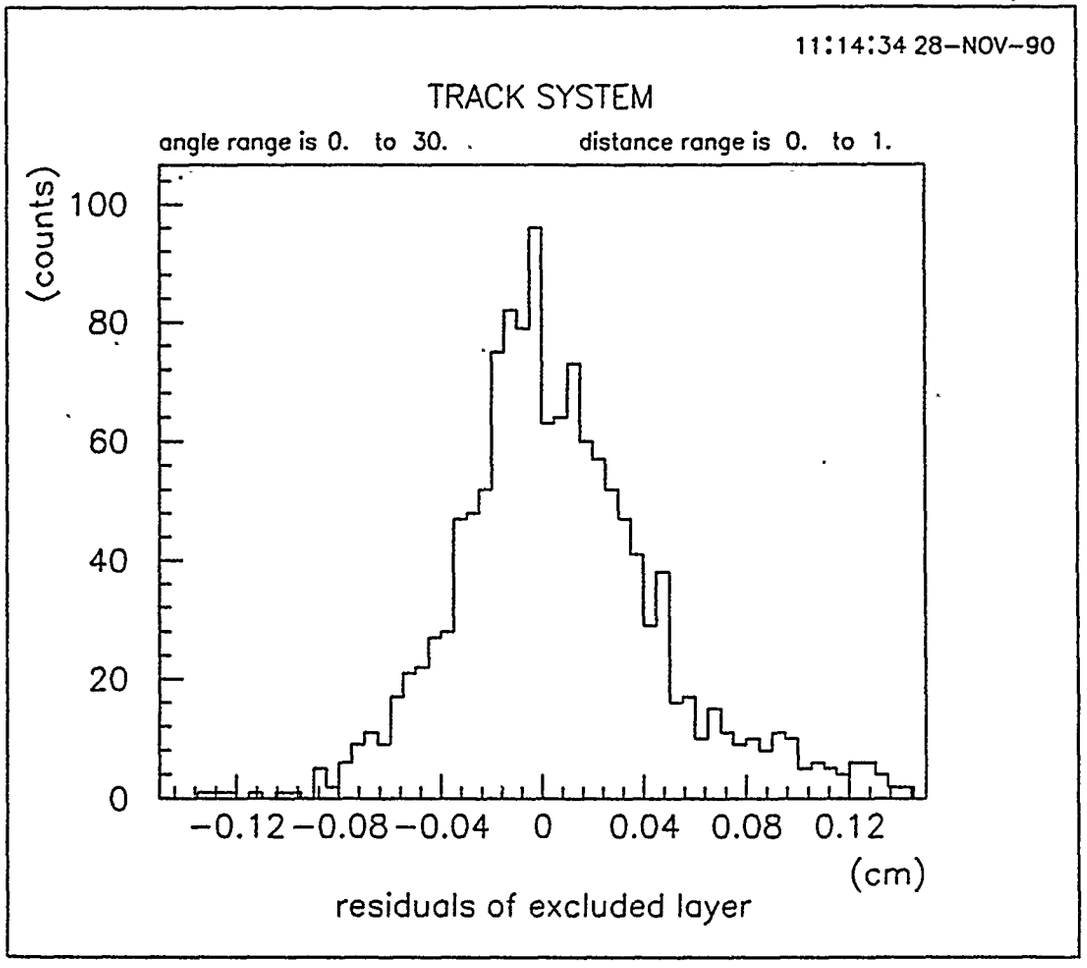

Fig. 36. Excluded Layer Residual Histogram for Argon:Ethane Run at B = 1.5.

Interpretation of Results

Studying the XTPLOTs for the helium:argon:ethane mixture indicates that the drift time at B=0 varies little from that at B=1.5 T. For example, without a magnetic field, at a distance of six millimeters from the sense wires, the drift time is approximately 247 ns. In comparison, at B=1.5T, the drift time at six millimeters is approximately 290 ns. This amounts to a decrease in velocity of roughly 17.4 percent.

When studying the (50:50) argon:ethane (a noticeably faster gas) mixture, at B=0 the drift time at six millimeters is about 130 ns. In the magnetic field, the drift time at six millimeters is roughly 210 ns. The difference in this velocity value is 61.5 percent slower!

To understand why such a difference exists, it is necessary to compare these results with the literature. Piesert and Sauli [Ref. 9] provide drift velocity curves for varying percentages of helium:ethane in figure 37.

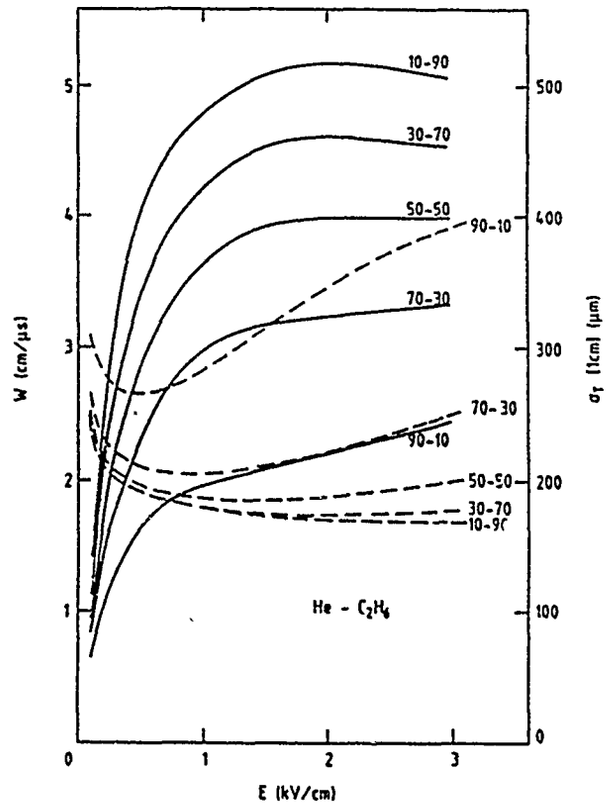

Figure 37. Drift Velocity of Helium and Ethane [Ref. 9].

Their mixture of 70:30 is approximately the same ratio as the 63:18.5 (neglecting the argon) in our mixture. Including the argon percentage in the mixture gives a ratio of 81.5:18.5, or roughly 80 percent helium and argon (where I combine the noble gases as a single gas entity) to 20 percent ethane.

A comparison of drift velocities at 2 keV/cm is as follows: 3.2 cm/μs for 70:30 helium:ethane [Ref. 9] versus our value of 2.4 cm/μs for 80:20 noble gases to ethane. Piesert and Sauli also show a drift velocity of approximately 2.2 cm/μs for a mixture of 90:10 helium:ethane. An approximation for the drift velocity of 80:20 helium:ethane, obtained by extrapolation between 70:30 and 90:10, is 2.7 cm/μs. Thus, the helium:argon:ethane mixture is 11% slower than the 80:20 mixture. This value is within a 20% difference of drift velocities given in other references and appears to be very reasonable.

As expected, helium accounts for the decreased velocity of the mixture. This reduction is what manifests the lessened effect of the magnetic field. With the Lorentz force, $\mathbf{F} = q(\mathbf{E} + \mathbf{v} \times \mathbf{B})$ the velocity of the electrons is "crossed" with the magnetic field. With a smaller velocity, the magnitude of vB is proportionately smaller.

To understand the effect of the magnetic field on helium, recall that the effect of a magnetic field **H** applied in a direction perpendicular to the electric field is given as follows:

$$w_M = \frac{w}{\sqrt{1 + \omega^2\tau^2}}, \quad \text{with} \quad \omega = \frac{eH}{m} \quad \text{and} \quad \tan \alpha_H = \omega \tau. \qquad (4.33)$$

With the expression, $\tau = \frac{2mw}{eE}$, it is apparent that magnetic drift velocity decreases as the denominator increases. With the magnetic field perpendicular to the electric field, the electrons initially move in a linear path which is dominated by the electric field. As the velocity increases, magnetic field dominates this motion and a cycloidal

path ensues. Drift occurs as the particles accelerate due to the electric field and are simultaneously pulled into a cycloidal path. This occurs until a collision takes place between the electrons and other molecules. For the overall motion in a magnetic field at a strength of 1.5 Tesla [Ref. 15], the electrons become slower and consequently the drift time increases.

Table 2 gives additional values for the mean free path and drift velocity for electrons in gases of interest [Ref. 19, 20]. As mentioned in chapter four, the drift velocity w, is dependent on the mean free path of the electron. The helium atom is much smaller than an ethane molecule or an argon atom.

Gas	Mean Free Path	Drift Velocity
Helium	2.8×10^{-5} cm	1.3×10^{6}cm/sec
Argon	1.0×10^{-5}	0.8×10^{6} cm/sec
Ethane	(O) 1.0×10^{-5}	5.4×10^{6}cm/sec

Table 2. Kinetic Properties of Gases of Interest.

The mean free path for helium is nearly three times that of argon and ethane. The average collision time for helium is roughly 2.2×10^{-11} seconds compared to 1.25×10^{-11} seconds for argon and 1.85×10^{-12} seconds for ethane. Ethane, being a "squishy" organic molecule compared to the noble gases of argon and helium, experiences an inelastic collision with the electrons. On the other hand, helium and argon undergo elastic collisions with the electrons. The net result is that the ethane molecule is able to continue its direction of drift after collision with an electron whereas the noble gases continue to bounce around after their collisions with electrons. By decreasing the amount of ethane available for collisions, and increasing the concentration of helium, the gas mixture on the whole becomes slower. Therefore, a slower drift time in the magnetic field can be attributed to a combination of an

increased average collision time for the three gases and a higher concentration of helium in a 3.4:1:1 ratio.

With regard to the analysis of the data and its corresponding results, some discussion on the least squares fit for a track is in order. Without a magnetic field, the assumption of the track as a straight line is correct. However, as shown in chapter four and displayed in the results, a high magnetic field of 1.5 Tesla will bend the track to one that closely resembles an arc. The motion of a particle with charge q in a magnetic field is stipulated by [Ref. 3]

$$\frac{dp}{dt} = \frac{q}{c} vXB. \tag{6.2}$$

The momentum is related to the magnetic field B and the radius of curvature by

$$p = 0.2998B\rho \tag{6.3}$$

where momentum is given in terms of GeV/c, the magnetic field in Tesla, and the radius in meters. Figure 38 [Ref. 3] shows the relation of the radius of curvature ρ, the chord l, and the sagitta s of a circular segment.

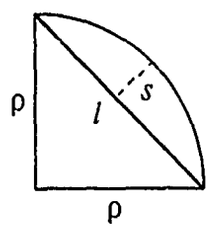

Fig. 38. A Circular Arc Showing the Radius, Chord and Sagitta.

These geometrical components of a circle are related by the following expressions

$$\rho = \frac{l^2}{8s} + \frac{s}{2} \cong \frac{l^2}{8s}. \tag{6.4}$$

It is estimated that for a 2 GeV particle, the bend in the track is approximately an arc

with a radius of two meters. Using the height of the chamber, the chord $l \cong 0.16$ m and with the approximate expression for the radius, the sagitta is approximately 1.6 mm or 1600 μ.

Therefore, a best fit line through an arc would experience a significant error at the top, middle and bottom portions of the track. Conversely, at the points where the track and the least squares fit intersect, the resolution would be that of the width of the line. In other words, the overall resolution for six layers within the chamber in a magnetic field is calculated as a root mean square value of each experimental point and the average value. One means of checking the resolution would be to examine the resolution of a different excluded layer such as layer two or four in the drift chamber. These two layers are closest to the intersection points of a straight line fit through the arc.

CHAPTER VII

CONCLUSION

The goal of this experiment was to examine a gas mixture suitable for the drift chambers in a Large Acceptance Spectrometer. Helium:argon:ethane was chosen as a candidate for examination. Specific questions were :

(1) Can a gas that was dominated by helium provide comparable resolution for the drift chamber when compared to a commonly used mixture of (50:50) argon:ethane?

(2) What is the effect of a constant high magnetic field using this helium dominated gas mixture?

Results obtained from comparing helium:argon:ethane in a ratio of 63:18.5:18.5 show that the residuals are very comparable to that of 50:50 argon:ethane. Accordingly, the mixture provides the necessary resolution for Large Acceptance Spectrometers and takes advantage of the decreased multiple scattering property of helium. Although this mixture is significantly slower, this noted difference in drift velocity reveals an important factor: the magnetic field does not effect helium as much as it does heavier gases such as argon and ethane.

The difference in drift velocity of the two mixtures is remarkable. The helium:argon:ethane mixture decreased approximately 17.4 percent whereas the argon:ethane mixture decreased approximately 61.5 percent. This difference is apparent in the average collision times of the two mixtures. With the helium dominated mixture, the collision time is approximately ten times less. However, with the decrease in the concentration of ethane, the available number of molecules which undergo inelastic collision is proportionately less. Therefore, the mixture becomes slower

because of the increased number of atoms which experience elastic scattering.

The optimum gas mixture for a drift chamber is very dependent on the application of the chamber. For proposed large acceptance spectrometers such as the CEBAF Large Acceptance Spectrometer (CLAS) or Bates Large Acceptance Spectrometer Torroid (BLAST), accurate spatial resolution is a necessary specification. The current designs of these spectrometers require large surrounding magnetic fields. In order to further attain effective resolution in areas both in and out of the magnetic field, the results of this experiment suggest that a slow drift velocity gas mixture of helium:argon:ethane can meet operational requirements.

The results obtained from this experiment indicate that helium dominated gas mixtures can be relatively unaffected by high magnetic fields. Future work in this area may suggest that by using a more effective quencher such as dimethyl ether (a slow, cool gas), even greater percentages of helium can be used in a gas mixture to take full advantage of helium's impassive properties in magnetic fields. With regard to the curved tracks, close study on the resolution for each layer is required in order to attain curvature from the six layers for a track. This will also require detailed work on developing an appropriate velocity function as well as learning more about ion pair diffusion. Finally, by making the transport theory correlate to the experimental results, the parameters such as diffusion and drift velocity of helium dominated gas mixtures can be coded into software programs such as GARFIELD. By doing so, "what if" analysis on drift chamber designs, field strengths, cell geometries etc. can be accomplished in an inexpensive manner.

BIBLIOGRAPHY

1) F. Sauli, Principles of Operation of Multiwire Proportional and Drift Chambers, CERN Report 77-09, 1977.

2) W.R. Leo, Techniques for Nuclear and Particle Experiments A How to Approach, (Berlin: Springer-Verlag, 1987), 119 - 143.

3) R. Fernow, Introduction to Experimental Particle Physics, (Cambridge, Cambridge University Press, 1990), 30 - 47, 205 - 252, 324-328.

4) R. Veenhof, revised by M. Gukes and K. Peters, GARFIELD, A Drift-Chamber Simulation Program, (Institut für Physik, Mainz, 1987)

5) S. Christo, Computer Aided Design Drawing "CEBAF Gas Test Wire Chamber Windows", April 1990.

6) Department of Energy Semi-Annual Review, "CEBAF End Station B", September 1990, Section G

7) S. Christo, Computer Aided Design Drawing "CEBAF Gas Test Wire Chamber Endplates", April 1990.

8) K. Kleinknecht, Detectors for Particle Radiation, (Cambridge, Cambridge University Press, 1986) pp 22-52.

9) A. Piesert and F. Sauli, Drift and Diffusion of Electrons in Gases: A Compilation (with an Introduction to Computer Programs), CERN Report 84-08, 1984

10) V. Palladino and B. Sadoulet, Application of Classical Theory of Electrons in Gases to Drift Proportional Chambers, Nuclear Instruments and Methods 128 (1975) 323-335.

11) H. W. Fulbright, Ionization Chambers in Nuclear Physics, Handbuch der Physik XLV Nuclear Instrumentation II, edited by S. Flügge, (Berlin, Springer-Verlag (1958) 1-51.

12) W. Braker and A. Mossman, Matheson Gas Data Book Fifth edition, (East Rutherford, N.J. (1971) pp 27,231,273.

13) G. Schultz and J. Gresser, A Study of Transport Coefficients of Electrons in some Gases Used in Proportional and Drift Chambers, Nuclear Instruments and Methods 151 (1978) 413-431.

14) W. De Boer et al., Performance of Drift Chambers without Field Shaping in High Magnetic Fields, Nuclear Instruments and Methods 156 (1978) 249-256.

15) B. Sadoulet and A. Litke, Behavior in Magnetic Field and Spatial Resolution of a Drift Chamber without Electric Field Shaping, Nuclear Instruments and Methods 124 (1975) 349-357.

16) S. Behrends and A.C. Melissinos, Properties of Argon-Ethane/Methane Mixtures for Use in Proportional Counters, Nuclear Instruments and Methods 188 (1981) 521-534.

17) W. Zimmerman et al., Helium-Propane as Drift Chamber Gas, Nuclear Instruments and Methods in Physics Research A243 (1986) 86-90.

18) M. Mestayer and S. Zhou, TRACK_OFFLINE: A FORTRAN Drift Chamber Track Program, CEBAF October 1990.

19) T. L. Cottrell and Isobel C. Walker, "Drift Velocities of Slow Electrons in Polyatomic Gases", Transactions of the Faraday Society, vol 61, (1965), pps 1585-1593.

20) A. von Engel, Ionization in Gases by Electrons in Electric Fields, Handbuch der Physik XXI Nuclear Instrumentation II, edited by S. Flügge, (Berlin, Springer-Verlag (1950) 542.